U. S. AIR FORCE

PROJECT RAND

RESEARCH MEMORANDUM

MINIMUM-WEIGHT DESIGN OF SANDWICH PANELS

L. E. Kaechele

RM-1895

ASTIA Document Number AD 133011

22 March 1957

Assigned to _____

This is a working paper. It may be expanded, modified, or withdrawn at any time. The views, conclusions, and recommendations expressed herein do not necessarily reflect the official views or policies of the United States Air Force.

The RAND Corporation
1700 MAIN ST. • SANTA MONICA • CALIFORNIA

SUMMARY

A structural design method is presented for determining the optimum configuration of flat, simply-supported sandwich panels under uniaxial compression, when the load, width, and stress-strain curves for the face material are given, with side conditions on the maximum allowable face stress (or strain) and on core strength or density. Application to square- and hexagonal-cell honeycomb core panels is shown, and elevated temperature effects are briefly discussed.

The method can be utilized to evaluate the weight efficiency of various materials. An example comparison is given which indicates that a significant weight advantage may be obtainable by use of titanium in the form of sandwich panels. In the region of low loading intensity, titanium sandwich panels appear to be about 10% lighter than aluminum sandwich panels, 25% lighter than stainless steel sandwich panels, and from 25 to 50% lighter than conventional aluminum sheet-stiffener panels, even at room temperature.

Further experimental work desirable for determining whether this potential can be realized is outlined.

CONTENTS

SUMMARY iii

Section

I. INTRODUCTION 1

II. ANALYTICAL WORK 3

III. DESIGN EQUATIONS 7

IV. DISCUSSION. 19

Comparison of Materials and Types of Construction 19
Experimental Work 24
Suggestions for Further Experiments 27
Extension of Method 25

Apendix

A. CORE PROPERTIES 31

B. ADHESIVE WEIGHT 37

C. APPROXIMATION FOR ORTHOTROPIC CORES 39

D. WRINKLING 45

E. MONOCELL BUCKLING 49

LIST OF SYMBOLS 51

REFERENCES. 53

FIGURES

1. Stress versus structural index curves for aluminum honeycomb panels 14

2. Equivalent stress versus structural index curves for aluminum honeycomb panels 15

3. Compressive stress-strain curve, 7075-T6 aluminum, room temperature 16

4. Envelope curves for aluminum honeycomb panels 18

5. Equivalent stress comparison of sandwich and sheet-stiffener construction 20

6. Relative weight comparison of sandwich and sheet-stiffener construction 22

7. Compressive stress-strain curves, room temperature 23

8. Comparison of theoretical curves and results of Boeing tests . . . 25

9. Method of investigating effects of plasticity 27

10. Method for checking wrinkling stress 28

11. Comparison of theoretical and experimental values of apparent core density 32

12. Reference axes for hexagonal cells 33

13. Comparison of theoretical and experimental values of core shear moduli 35

14. $\sigma_{eq} - q/b$ curves for bonding weight discussion 38

15. Non-dimensional buckling curves 40

16. Non-dimensional buckling curves for evaluation of approximation discussed in Appendix C 42

17. Wrinkling stress versus t/d for faces supported by honeycomb cores 47

18. Monocell buckling stress versus q/d 50

19. Panel geometry 51

I. INTRODUCTION

Structural elements whose function is the transmission of compressive loads (e.g., upper wing-surface panels) frequently must do this at stresses which are lower than those imposed by material limitations, because of the necessity for a configuration which is stable enough to prevent buckling. The problem of designing a configuration which will be stable at high stress is particularly acute in the region of low loading intensity (small loads and/or large transmission or application lengths). Expansion of the cross section is an obvious means of improving stability, and several types of construction utilizing this principle are in use, e.g., a skin with integral or attached stiffeners, two skins with stiffening webs or corrugation between them, and sandwich construction in which two skins or faces are separated and more or less continuously supported by a low-density core material.

The idea of sandwich construction is not new -- use in airplanes is reported as early as 1919,[1] and in the past ten or fifteen years a considerable amount of theoretical work has been done on the analysis of this type of construction. However, there is little information available on the design aspect -- the choice of the best configuration when the load and over-all dimensions are known.

This investigation is concerned with the design problem for uniaxial compressive loading of simply-supported honeycomb-core sandwich panels. By a reformulation of analysis equations it presents a method of determining the configuration which results in the lightest panel weight for given loading, panel width, and side conditions on core properties and on maximum allowable strain. With this information the designer can compare the

strength and weight of sandwich construction with other types of construction and choose the best type for a given application. As might be expected, sandwich construction appears particularly advantageous in the region of low loading intensity.

II. ANALYTICAL WORK

The extension of ordinary plate theory to the stability problem for sandwich construction is complicated by the necessity of considering shear deflections, and further, by the orthotropic properties of some of the core materials in current use. Libove and Batdorf[2] included these effects in developing the energy expression and the differential equations for the flat orthotropic plate. Ericksen and March,[3] using an energy method, obtained a solution for the buckling load for flat sandwich panels with orthotropic cores, and orthotropic and unequal faces. Plantema[4] presented a buckling equation obtained from the method of partial deflections for a rectangular, infinitely long, simply-supported* flat sandwich panel with equal isotropic faces and orthotropic core. For these conditions, the energy, partial deflection, and differential equation methods are equivalent, and the buckling load for uniaxial compression is

$$q = \frac{\pi^2 B}{b^2} \cdot \frac{\left[\lambda s_x + a\,(r + \lambda)\right](1 + \lambda)^2}{\lambda + \lambda^2 r + \lambda^2 s_x + a\lambda\,(r + \lambda) + ar\,(1 + \lambda)^2/s_x} \quad \text{for } s_x \geq 1/r \qquad (1)$$

$$q = \frac{\pi^2 B s_x}{b^2} \quad \text{for } s_x \leq 1/r^{**} \qquad (2)$$

---

*Inclusion of shear deflections introduces a shear boundary condition in addition to the conditions of ordinary plate theory. For simple support, this condition is either zero twisting moment at the edge or zero shear strain in a plane normal to the plate and parallel to the edge. The latter condition, which corresponds to the presence of edge stiffeners, will be used here.

**This is strictly true only for $r \geq 0.69$, but it appears sufficiently accurate for lower values of r. See discussion in Ref. 4, p. 30.

The customary assumptions have been made here, viz., the in-plane stiffness of the core is much less than that of the faces, so that bending moments are due only to stress in the faces; the shear stresses in the faces in a direction perpendicular to the plate are negligible; and the moment of inertia of the individual faces about their own centroid is negligible compared with that of the faces about the centroid of the plate. These assumptions are conservative and appear generally realistic, with the exception of the final one, which may give overly conservative results in cases where the shear rigidity and bending rigidity are nearly equal. The solution for the infinitely long plate may be used for finite plates with a length-to-width ratio of about 3 or more, with slightly conservative results.

In Eq. (1) the proper wavelength is that which minimizes q. However, setting $\partial q/\partial \lambda$ equal to zero yields a rather unwieldy cubic equation in λ, and it is probably simpler to determine λ by trial, as Plantema has done for several values of r, the ratio of the apparent core shear moduli in the directions parallel and perpendicular to the loading direction.

If the core is isotropic, or cylindrically aeolotropic, (e.g., square-cell honeycomb), r = 1, and Eq. (1) simplifies to

$$q = \frac{\pi^2 B}{b^2} \cdot \frac{s\,(1 + \lambda)^2}{\lambda s + \lambda + 1} \tag{3}$$

which agrees with the solution given by Bijlaard[5] and, aside from a decrease in shear rigidity arising from neglect of the thickness of the faces, with that given by Hoff.[6] Minimizing this expression with respect to λ gives

$$\frac{\partial q}{\partial \lambda} = \frac{\pi^2 Bs}{b^2} \cdot \frac{(1 + \lambda)\left[\lambda (s + 1) - (s - 1)\right]}{(\lambda s + \lambda + 1)^2} = 0 \qquad (4)$$

from which

$$\lambda = \frac{s - 1}{s + 1} \text{ for } s \geq 1 \text{ and } \lambda = 0 \text{ for } s \leq 1 \ ^*$$

Thus

$$q = \frac{\pi^2 B}{b^2} \cdot \frac{4s^2}{(1 + s)^2} \text{ for } s \geq 1 \qquad (5)$$

and

$$q = \frac{\pi^2 Bs}{b^2} \text{ for } s \leq 1 \qquad (6)$$

Seide and Stowell[7] also give this result, but again with the lower value of shear rigidity mentioned above.

In view of the difficulty involved in obtaining an expression for the buckling load independent of λ in the orthotropic case, it appears desirable to explore the possibility of obtaining an approximation in a more tractable form. One method of doing this is indicated by the form of the buckling load expression when s is large enough to make the effects of shear rigidity unimportant. The panel then buckles with a half wave-length equal to its width, i.e., $\lambda = 1$. Putting this value of λ in Eq. (1), the buckling load for the orthotropic case then becomes

$$q = \frac{4\pi^2 B}{b^2} \cdot \frac{\left[s_x + a (r + 1)\right]}{1 + r + s_x + a (r + 1) + 4ar/s_x} \qquad (7)$$

---

*Zero wave length arises from the assumption that the faces are membranes with no bending rigidity. In general, the error introduced by this assumption is small. If the bending rigidity of the faces is considered, the buckling wave length is always greater than zero.

$$q = \frac{4\pi^2 B}{b^2} \cdot \frac{\left[1 + a\,(r + 1)/s_x\right]}{(1 + r)/s_x + 1 + a\,(r + 1)/s_x + 4ar/s_x^2} \tag{8}$$

Since we are considering only large values of s_x, we may neglect terms in a. Hence,

$$q \simeq \frac{4\pi^2 B}{b^2} \cdot \frac{1}{(1 + r)/s_x + 1} \tag{9}$$

For the isotropic case, setting $\lambda = 1$ in Eq. (3) gives

$$q \simeq \frac{4\pi^2 B}{b^2} \cdot \frac{1}{2/s + 1} \tag{10}$$

Therefore, if we define an equivalent s by

$$s_{eq} = \frac{2s_x}{1 + r} \tag{11}$$

we can treat the orthotropic case by using the equations developed for the isotropic case. This definition is tantamount to defining an effective core shear rigidity,

$$G'_{c\ eff} = \frac{2\,G'_{cx}\,G'_{cy}}{G'_{cx} + G'_{cy}} \tag{12}$$

The validity of this approximation is treated in Appendix C.

III. DESIGN EQUATIONS

The discussion thus far has dealt only with analysis, i.e., with methods of computing the buckling load for given configurations and materials. The design problem -- determination of configuration when the load is given -- requires a reformulation of the analysis equations. For the type of structure considered here the primary design parameters are the load q and the width b, and the structural index is q/b. Analogous to the procedure for homogeneous isotropic plates, the stress at which buckling occurs can be plotted against q/b. (Two additional parameters, the core shear modulus and the face-to-core thickness ratio, must be considered in sandwich construction.) Then, given q and b, the buckling stress can be found and the proper thickness of core and face determined. (If b is not prescribed, e.g., if spar spacing can be varied, the effect of width variations on the over-all configuration and weight can be assessed.)

The stress-structural index relationship can be derived from Eq. (5):

$$q = \frac{4\pi^2 B}{b^2} \cdot \frac{s^2}{(1+s)^2} = \frac{4\pi^2 Bs}{b^2} \cdot \frac{1}{s\,(1+1/s)^2} \tag{13}$$

or, with

$$s = \frac{b^2}{\pi^2 B} \cdot \frac{(c+f)^2 G'_c}{c}$$

where G'_c may also be $G'_{c\ eff}$ as given by Eq. (12),

$$q = 4c\,(1+k_t)^2\, G'_c \frac{1}{s\,(1+1/s)^2} \tag{14}$$

In this form, q is symmetrical in s and 1/s, and it must be remembered that this expression is valid only for $s \geq 1$.

Then

$$\sigma = q/2f = \frac{2\,(1 + k_t)^2}{k_t}\, G_c' \cdot \frac{1}{s\,(1 + 1/s)^2} \tag{15}$$

and

$$1 + 1/s = \sqrt{\frac{2\,(1 + k_t)^2\, G_c'}{\sigma\, k_t}}\ \sqrt{1/s} \tag{16}$$

Then writing

$$s = \frac{b^2}{\pi^2 B}\,\frac{(c + f)^2 G_c'}{c} = \frac{b^2\,(c + f)^2 G_c'\, 2\,(1 - \nu^2)}{\pi^2 E_f cf\,(c + f)^2} =$$

$$\frac{2\,(1 - \nu^2)\, G_c'}{\pi^2 E_f} \cdot \frac{b^2}{cf}$$

or, since $f = q/2\sigma$ and $c = q/2k_t\sigma$

$$s = \frac{8\,(1 - \nu^2)\, G_c'}{\pi^2 E_f}\, k_t\, \frac{\sigma^2}{(q/b)^2}$$

and we may write Eq. (16) as

$$1 + \frac{\pi^2 E_f}{8\,(1 - \nu^2)\, G_c'\, k_t} \cdot \frac{(q/b)^2}{\sigma^2} = \sqrt{\frac{2\,(1 + k_t)^2 G_c'}{k_t \sigma}}\ \sqrt{\frac{\pi^2 E_f}{8\,(1 - \nu^2)\, G_c'\, k_t}} \cdot \frac{q/b}{\sigma} \tag{17}$$

This quadratic may then be solved to give

$$q/b = \frac{2\,(1 + k_t)\,\sqrt{1 - \nu^2}\,G'_c\sqrt{\sigma}}{\pi\sqrt{E_f}} \left\{ 1 - \sqrt{1 - \frac{2\sigma k_t}{G'_c\,(1 + k_t)^2}} \right\} \qquad (18)$$

(The minus sign must be used before the radical to satisfy the condition $s \geq 1$.)* The radical can be expanded in a series in order to observe more readily the effect of the parameters G'_c and k_t. This gives

$$q/b = \frac{2\,(1 + k_t)\,\sqrt{1 - \nu^2}\,G'_c\sqrt{\sigma}}{\pi\sqrt{E_f}} \left\{ \frac{\sigma k_t}{G'_c\,(1 + k_t)^2} + \frac{1}{8}\left[\frac{2\sigma k_t}{G'_c\,(1 + k_t)^2}\right]^2 + \cdots \right\} \qquad (19)$$

It is then apparent that increasing G'_c or decreasing k_t will result in a lower value of q/b for a given stress, which is desirable from the standpoint of optimization, since this means a higher attainable buckling stress for a given q/b. However, both of these avenues tend to increase the weight of core relative to the weight of faces, and the effect on the total weight of the panel must be investigated. This may be done by considering an

---

*When $s \leq 1$, (or when $s_x \leq 1/r$ for the orthotropic case) $q = \frac{\pi^2 B s_x}{b^2} = \frac{(c + f)^2 G'_{cx}}{c} = (1 + k_t)^2 G'_{cx}$. This is the shear buckling load. The shear buckling stress, the highest attainable stress for given k_t and G'_{cx} (with bending rigidity of faces neglected) is

$$\sigma = q/2f = \frac{(1 + k_t)^2 G'_{cx}}{2 k_t} .$$

"equivalent stress", i.e., the stress that would exist in a solid plate of some reference material carrying the same load and having the same weight as the sandwich panel. From the first condition we have $\sigma_{eq}\, t_r = 2f\sigma$, and from the second, $t_r\gamma_r = 2f\gamma_f + c\gamma_c' + w_b$, where t_r is the thickness of the solid plate, w_b is the weight of all the face-to-core bonding material per unit area of sandwich panel, and γ_r, γ_f, and γ_c' are respectively the specific weights of the reference material, the face material, and the apparent specific weight of the core. Then

$$\sigma_{eq} = \frac{2f\sigma}{t_r} = \frac{2f\sigma}{2f\,\gamma_f/\gamma_r + c\gamma_c'/\gamma_r + w_b/\gamma_r}$$

$$= \frac{k_t}{k_t\,\gamma_f/\gamma_r + \gamma_c'/2\gamma_r + w_b/2c\gamma_r} \cdot \sigma \qquad (20)$$

Since it appears impossible at present to relate w_b directly to face or core thickness, the term w_b will be neglected, noting, however, that in some cases a significant decrease in equivalent stress may result if the weight of this bonding material is considered. Henceforth then, the equivalent stress is defined by

$$\sigma_{eq} = \frac{k_t}{k_t\,\gamma_f/\gamma_r + \gamma_c'/2\gamma_r} \cdot \sigma \qquad (21)$$

It is shown in Appendix B that under certain conditions neglect of w_b does not affect determination of the optimum configuration.

Extension of the above theory of elastic buckling to inelastic behavior appears to be possible by multiplying Young's modulus by a reduction factor, η. This has been suggested in several studies, but with considerable variance of opinion about the proper form of η.

Johnson and Semonian,[8] in one of the few studies of the design problem, assume that the value of η given by Stowell[9] for solid plates may be used in their buckling equation. The assumption that the core shear modulus and Young's modulus for the faces are reduced by the same factor is implicit in their derivation. If the core is assumed to remain elastic, the value of η may depend on the buckling wave length. Bijlaard[5] incorporates plasticity effects by a method he developed previously, and gives the buckling load (if the bending rigidity of the faces is neglected) as

$$q = \frac{\pi^2 B_s}{b^2} \cdot \frac{1 + \lambda}{1 + \frac{(1 + \lambda)s}{\eta_B}} \tag{22}$$

where

$$\eta_B = (1 + \nu^2) \left\{ \frac{1}{\lambda} \cdot \frac{1 + 3E_t/E_s}{2 - 4\nu + 3E_f/E_s - (1 - 2\nu)^2 E_t/E_f} + \right.$$

$$\frac{4\left[1 - (1 - 2\nu) E_t/E_f\right]}{2 - 4\nu + 3E_f/E_s - (1 - 2\nu)^2 E_t/E_f} + \frac{4}{2\nu - 1 + 3E_f/E_s} +$$

$$\left. \frac{4\lambda}{2 - 4\nu + 3E_f/E_s - (1 - 2\nu)^2 E_t/E_f} \right] \cdot \frac{\lambda}{(1 + \lambda)^2} \tag{23}$$

and E_t, E_s and E_f are the tangent, secant, and Young's moduli of the face material, and ν is Poisson's ratio for the face material. It is apparent that the λ which minimizes q in the plastic range cannot be determined simply as was done in Eq. (4). Seide and Stowell investigate the effect of plasticity and develop a rather complicated method of including this effect which also depends on buckling wave length.

Lack of experimental data necessitates a rather arbitrary choice of η and for reasons of simplicity η will be taken here as $\sqrt{E_t/E_f}$,* and E_f in the buckling equations is merely replaced by $E_f\eta$. It is thus assumed that the core remains elastic, and that the wave length which minimizes q can still be obtained from Eq. (4). It is also assumed that changes in ν in the plastic region may be neglected.

Now, writing

$$q/b = \frac{2\,(1 + k_t)\,\sqrt{1 - \nu^2}\,G_c'\sqrt{\sigma}}{\pi\sqrt{E_f\eta}}\left\{1 - \sqrt{1 - \frac{2\sigma k_t}{G_c'\,(1 + k_t)^2}}\right\} \qquad (24)$$

to include the effect of plasticity, the optimization problem can be considered. (Although we are considering the buckling stress to be a function of the structural index, writing the relationship in inverse form simplifies computation, since η is a function of stress.)

Ideally, if core material is available in any desired density and hence shear rigidity, and there is no maximum stress limitation, the optimum configuration is that at which the panel buckling stress is equal to the stress for the wrinkling type of failure (in which the individual faces buckle in short waves as plates supported by an elastic foundation). Flügge [11] has discussed the optimum design problem from this standpoint, assuming elastic behavior, and has presented diagrams in terms of dimensionless parameters from which optimum dimensions and core properties may be determined.

As is shown in Appendix D, the wrinkling stress for faces supported by presently available metallic honeycomb cores may be so high that it does not

*As shown in Ref. 10, this expression for η agrees quite well with that derived in Ref. 9 for the case of simply-supported solid flat plates.

appear reasonable to design for simultaneous buckling and wrinkling in all cases. Hence, the method presented here is constructed to permit optimization with respect to other side conditions: First, a limitation on the honeycomb core, determined by, for example, a requirement for adequate crushing strength for loads normal to the plate, or by availability, cost, or fabrication considerations; and second, a condition on the maximum allowable strain, or equivalently, a maximum allowable stress. Wrinkling can easily be included when necessary, as can a third type of instability, monocell wrinkling, in which the skin may buckle into or out of a cell, as a plate supported by the cell walls. The stress for this mode is a function of the cell size; theoretically it need not be considered, since for a given core density the cell size may be reduced sufficiently to eliminate monocell wrinkling. Again, practical considerations may necessitate inclusion of this effect.

Using Eq. (24), curves of σ versus q/b can be obtained as shown in Fig. 1, and with Eq. (21) these curves can be transformed to σ_{eq} versus q/b as in Fig. 2. These curves are for 7075-T6 aluminum alloy at room temperature, and aluminum is the reference material used in obtaining equivalent stress. The compressive stress-strain curve for this material is shown in Fig. 3. This curve was approximated with Ramberg-Osgood coefficients, and the problem was programmed for computation on a digital computer. The curves shown in Fig. 2 are for square cell honeycomb, with one value of t/d, viz. .012 (and therefore effective G_c', see Appendix A and Eq. (12)). Similar curves result if other values of t/d are used. In this case cut-off stresses are indicated which result in plastic strains of .002 and .01 in/in. Clearly, other values of maximum allowable strain could be used to determine the cut-off stress.

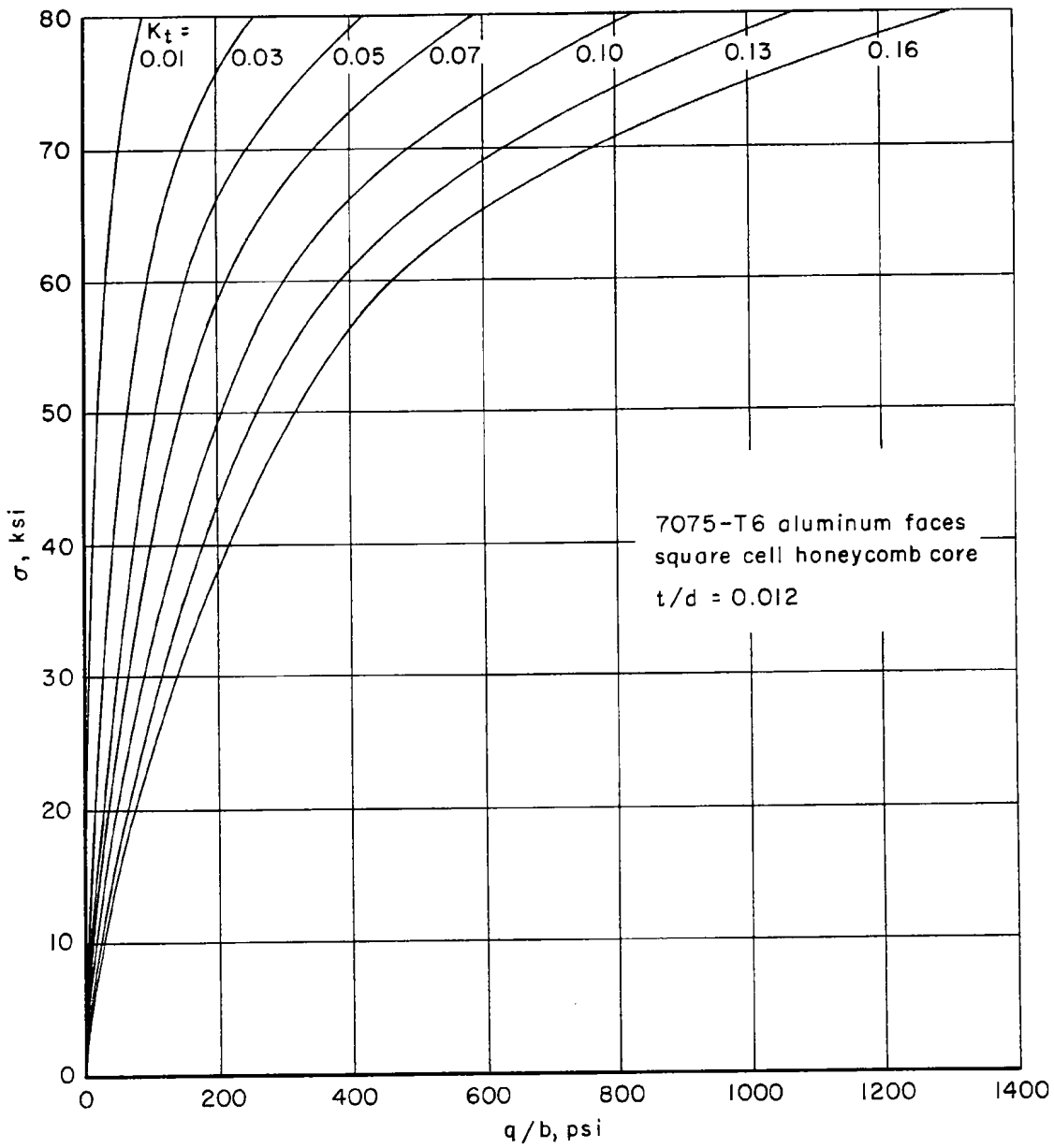

Fig. 1 — Stress vs structural index curves for aluminum honeycomb panels

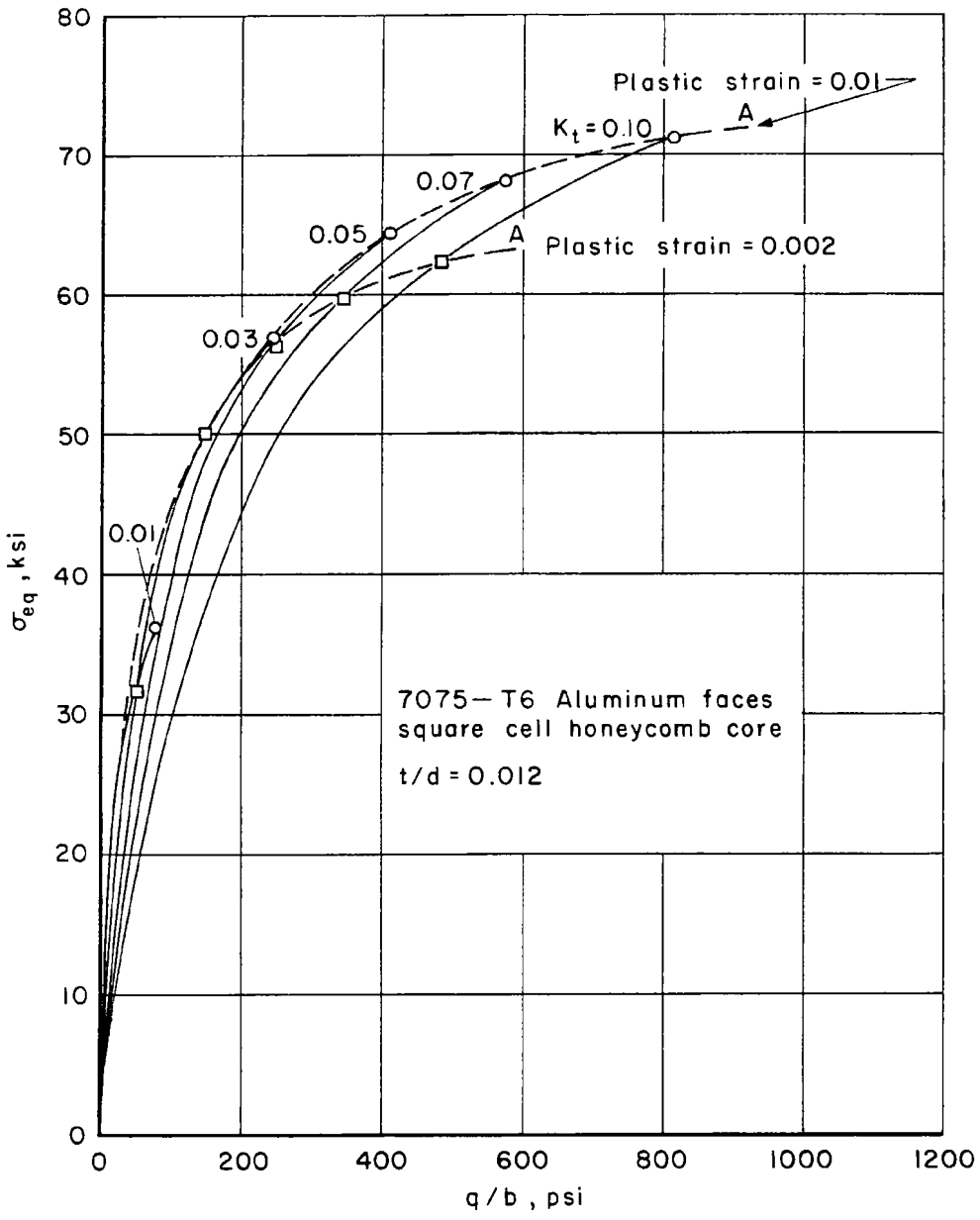

Fig. 2 — Equivalent stress vs structural index curves for aluminum honeycomb panels

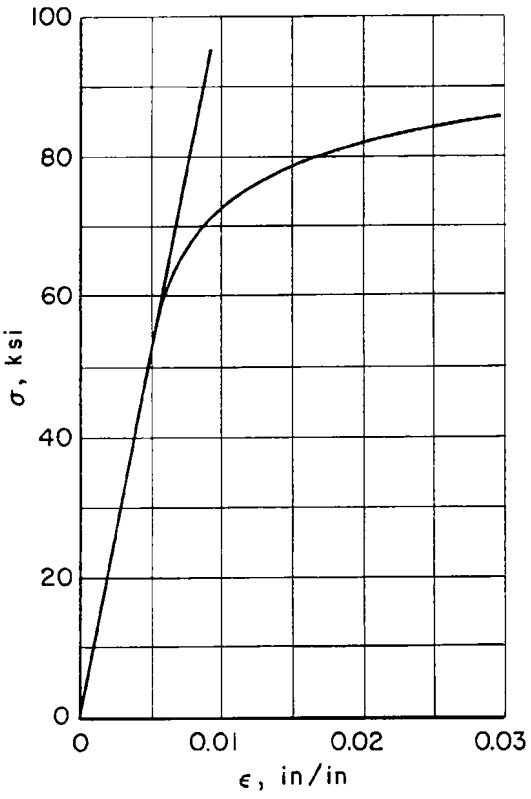

Fig. 3—Compressive stress-strain curve, 7075—T6 aluminum, room temperature

The effect on equivalent stress of decreasing k_t is shown in this figure by the intersection of the buckling curves for the lower values of k_t. In this region, lighter construction may result if the face stress at buckling is decreased and k_t increased.

To determine optimum configuration, it is apparent from Fig. 2 that envelope curves can be constructed, as curves A in that figure, passing through the points of maximum equivalent stress for a given value of cut-off stress, or, in the region where the curves intersect, tangent to the curves for the different values of k_t. Then, for a given q/b, the maximum attainable value of σ_{eq} can be found, as can the proper value of k_t, by interpolation if necessary. This information, with the core density and the density of the reference material, permits determination of the required face and core thickness.

If it appears that the wrinkling mode of failure should be taken into consideration, this may be done by terminating each buckling curve at a face stress equal to the wrinkling stress for the given face, core, and value of k_t. The design procedure would be unchanged whether the position of the envelope curve is determined by wrinkling stress or by a strain limitation.

Envelope curves for several values of t/d may be plotted together, as

shown in Fig. 4, and the resulting envelope of these curves indicates the "optimum" curve for the material considered, i.e., optimum in that it shows the highest equivalent stress (and therefore lightest weight) attainable for the given material, with the given stress limitation and range of t/d considered. For the lower values of t/d, the cut-off stress was assumed to be wrinkling stress as computed from the formula suggested in Appendix D.

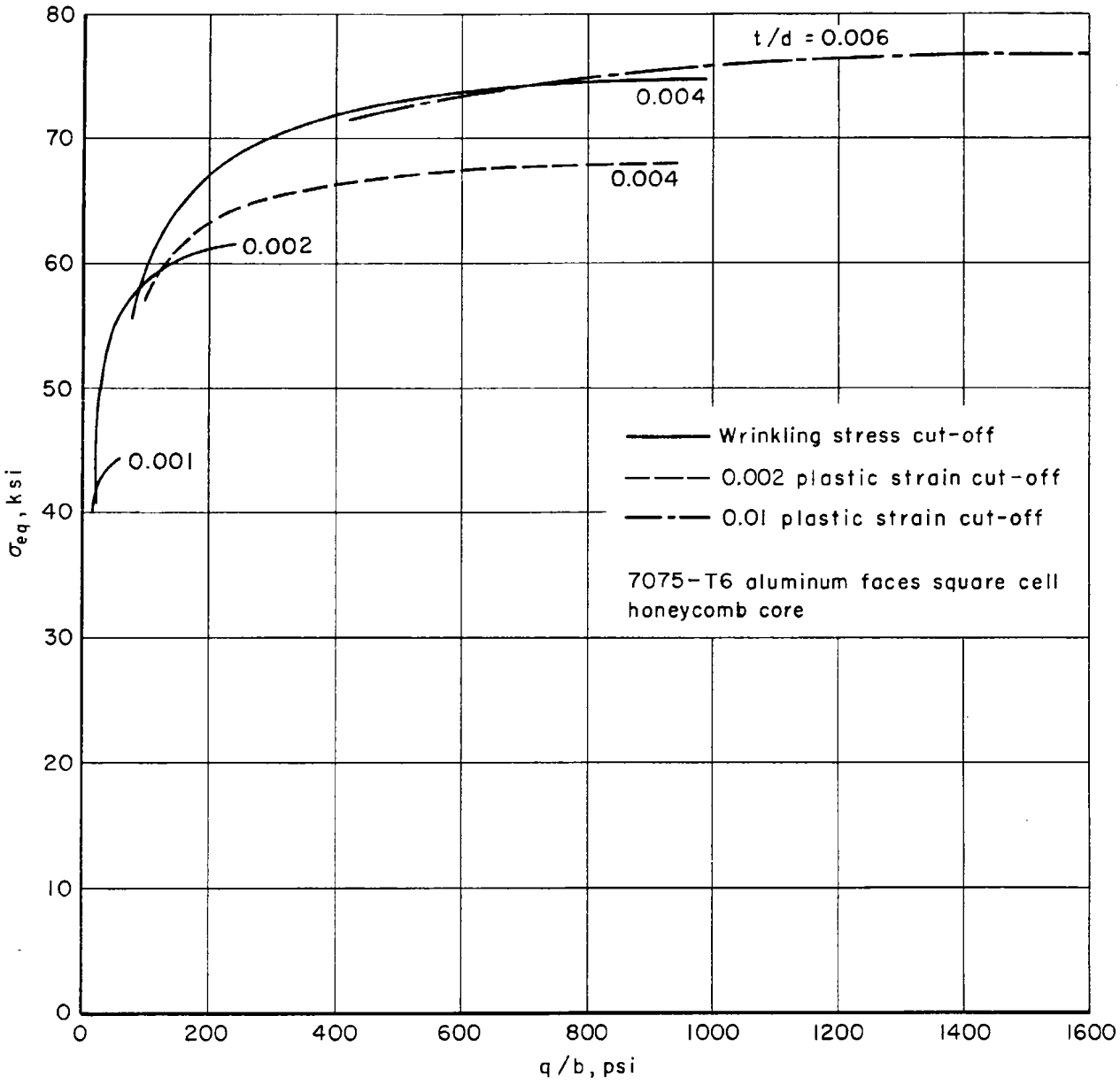

Fig. 4 — Envelope curves for aluminum honeycomb panels

IV. DISCUSSION

Comparison of Materials and Types of Construction

By utilizing the procedure outlined in the previous section, comparison of honeycomb panels constructed of different materials is possible. Such a comparison is shown in Fig. 5 for aluminum, beryllium, steel, and titanium sandwiches. Aluminum was the reference material used in determining equivalent stress. Because of the support given the faces by the core in a sandwich panel, it is possible to stress them to a high level, hence the strength of titanium can be utilized even at low levels of loading intensity. This effect is reflected in the attainable equivalent stress as shown in Fig. 5: at a structural index of 300 psi, the equivalent stress for titanium is 1.13 times that for aluminum, which means that the weight of a titanium panel would be 89% of the weight of an aluminum panel of the same width and carrying the same load.

Comparison of honeycomb sandwich with other types of construction, e.g., sheet stringer, can also be made. An example of this is shown by plotting optimum buckling curves for sheet-stiffener panels[12] with the honeycomb panel curves in Fig. 5. The structural index for sheet-stiffener panels is q/L_o, where q is again the load in lb/in and L_o is the effective pinned-end length of the panel. The difference in structural indices for the two types of construction (supports at spacing b are parallel to the loading direction for the sandwich and supports at spacing L are perpendicular to the loading direction for the sheet-stiffener panel) makes the comparison necessarily approximate. However, for the sake of a rough comparison, if it is assumed that setting b equal to L results in about the same total weight of supports, it is clear that for a given material, sandwich construction results in much

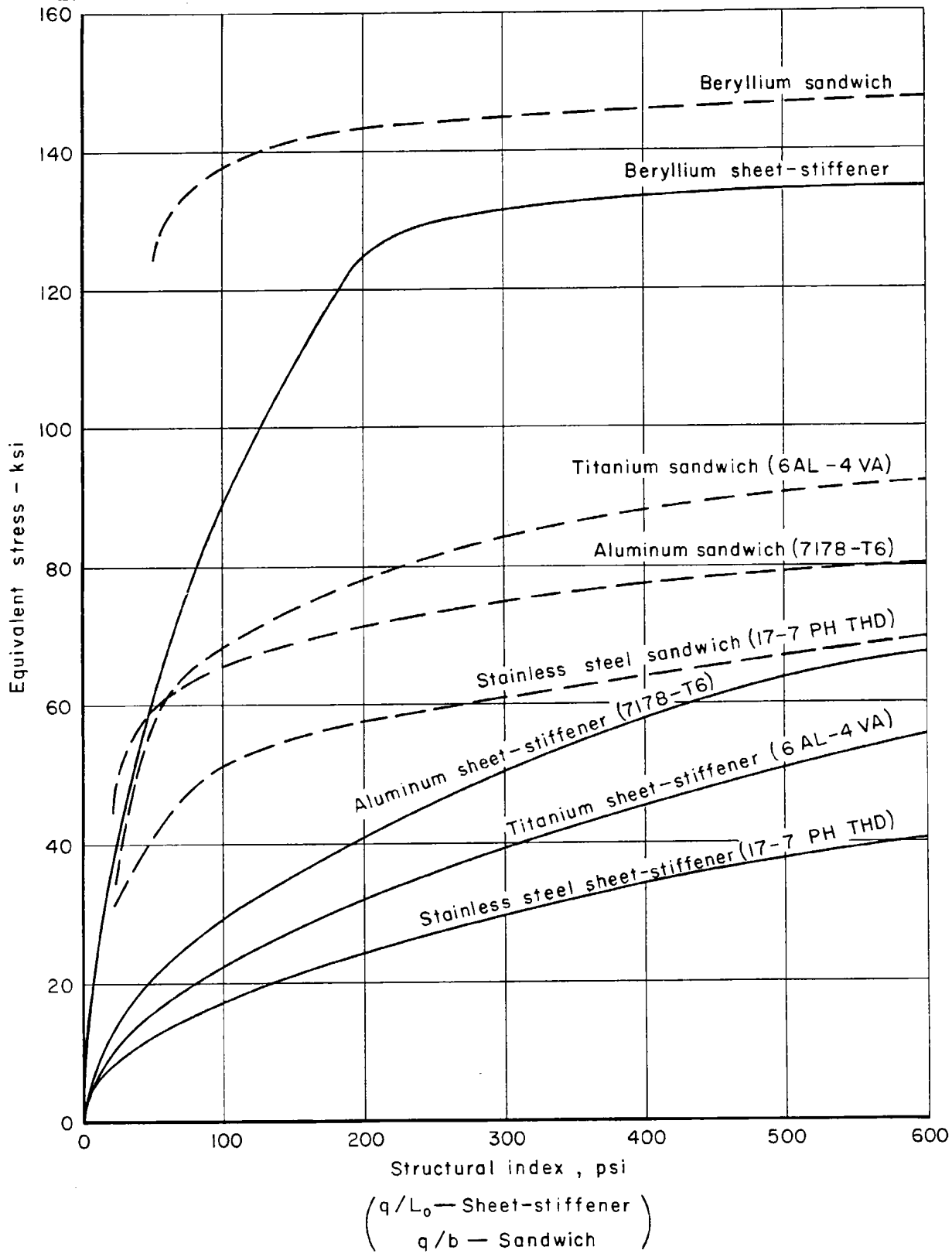

Fig. 5 — Equivalent stress comparison of sandwich and sheet-stiffener construction

lighter weight for low values of structural index. Alternatively, for a given q and for panels of the same weight in the two types of construction, the support spacing, b, for the sandwich panel can be considerably greater than the support spacing, L, for the sheet-stiffener panel.

The weight saving possible with the titanium sandwich is even more pronounced when compared with conventional aluminum sheet-stiffener construction. At a structural index of $q/b = q/L_o = 300$ psi, the titanium sandwich panel would weigh about 40% less than the aluminum sheet-stiffener panel.

An over-all picture of relative weights is shown in Fig. 6 where weights of sandwich and sheet-stiffener panels relative to the weight of an aluminum sheet-stiffener panel are shown. The weight advantage of honeycomb construction in regions of low structural index is clearly apparent in this figure.

The room-temperature compressive stress-strain curves used in obtaining the curves for the above comparisons are shown in Fig. 7. For each of the honeycomb panel curves, the core and face material were the same*, a range of t/d from .001 to .016 was considered (square cell honeycomb), and the cut-off stress was either the wrinkling stress (computed from the equation suggested in Appendix D) or the stress which produced a plastic strain of .01.

It is very important to remember that the level of the envelope curves for honeycomb panels depends strongly on the attainable face stress. The

---

*Since the modulus-density ratio is about the same for aluminum, titanium and steel, cores of these materials with the same density should have about the same elastic properties. Therefore, the curves in Fig. 5 would change very little if these core materials were interchanged, e.g., if titanium faces were used with aluminum or steel cores.

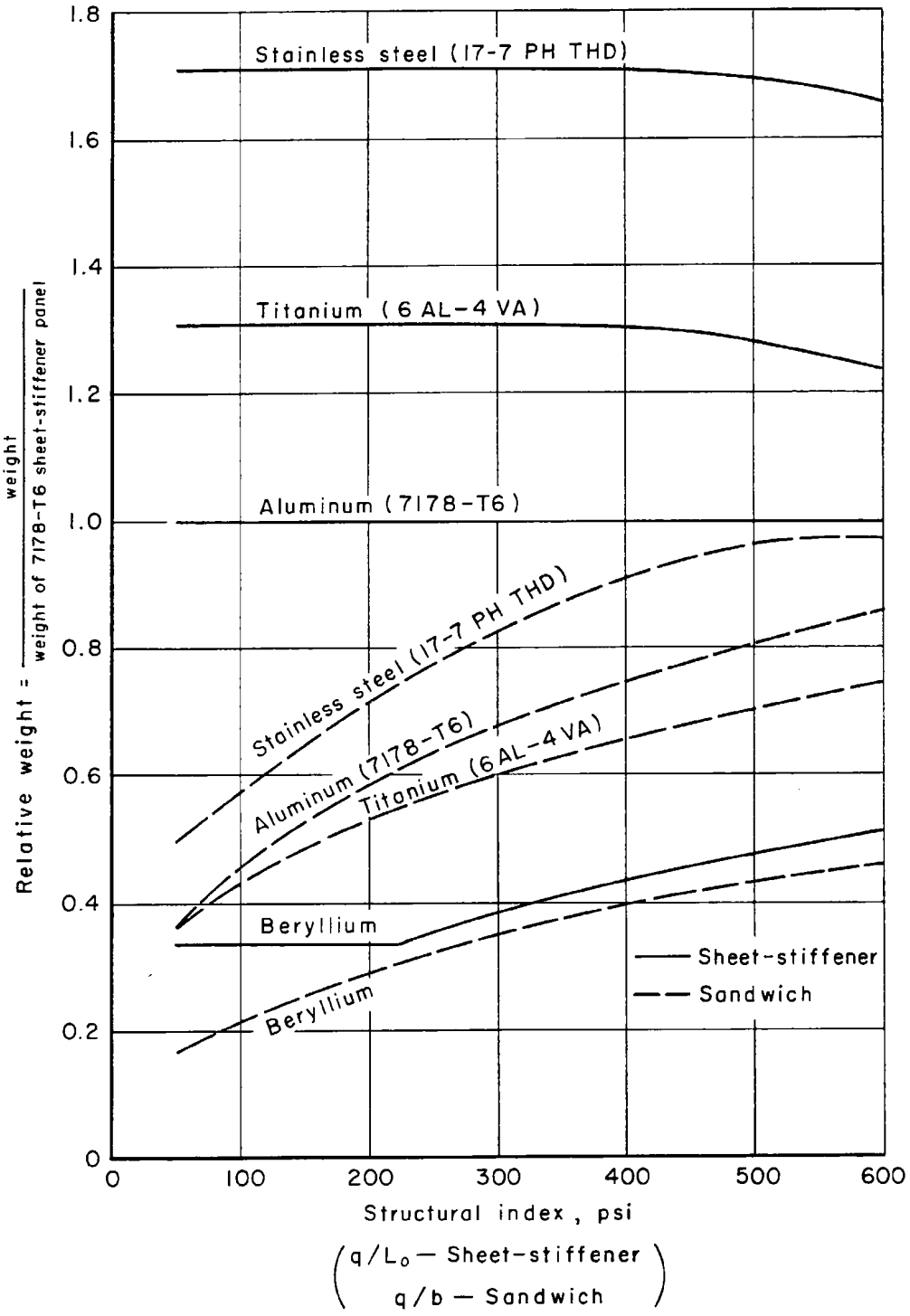

Fig. 6 — Relative weight comparison of sandwich and sheet-stiffener construction

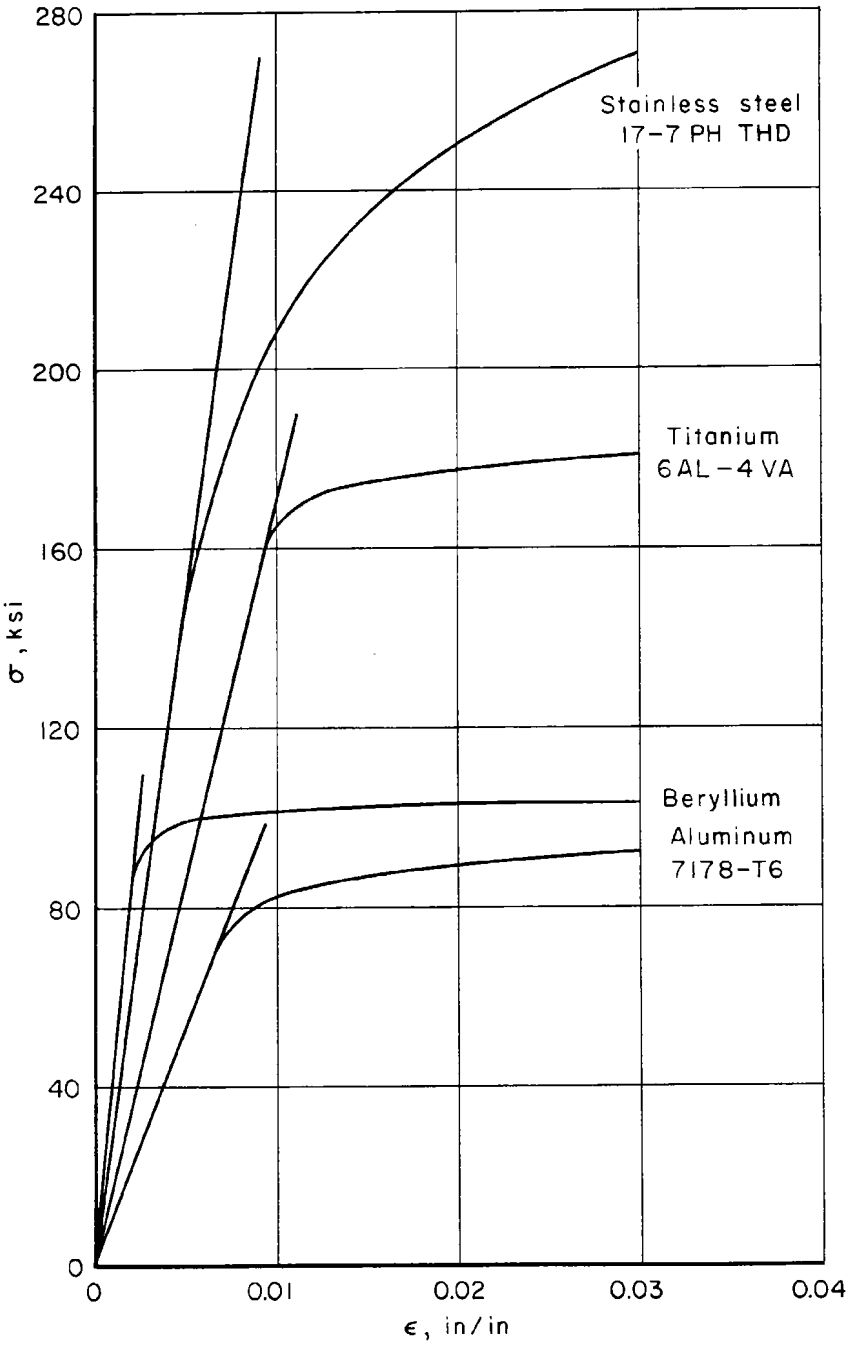

Fig. 7 — Compressive stress-strain curves, room temperature

magnitude of the cut-off face stress for a given strain limitation depends in turn on the stress-strain curve used. The curves in Fig. 7 are taken from laboratory tests and are not to be taken as guaranteed values for design purposes.

The other face-stress cut-off, wrinkling stress, also affects the level of envelope curves. This stress also depends on the stress-strain curve, but at present there is far too little information on wrinkling tests to predict the wrinkling stress with certainty.

If minimum gage requirements must be met, it may be necessary to reduce the cut-off face stress. That is, for a given q, the maximum face stress that can be obtained is $\sigma = q/2f_{min}$, where f_{min} is the minimum allowable face thickness. If this stress is below the cut-off stress determined by a strain limitation or by wrinkling, a new envelope must be plotted using the cut-off stress determined by the minimum gage limitation. Thus, for low values of q, a minimum gage requirement may markedly depress the attainable equivalent stress.

As discussed in Appendix B, bonding material weight may in some cases also reduce significantly the magnitude of equivalent stress.

Experimental Work

It should be emphasized that there are insufficient data available on metallic honeycomb-core sandwich-panel buckling tests to permit assurance in the use of design curves based on theoretical work. There are several factors which may, in practice, tend to depress the attainable strength level of honeycomb panels, e.g., irregularities in the faces, either present initially or produced during the bonding operation by variations in core thickness. The effect of irregularities may be related to the buckling wave

length. As noted elsewhere, the determination of the stress for the wrinkling type of instability is uncertain, as is the effect of inelastic behavior on primary buckling stress. However, a limited amount of experimental work on aluminum sandwich panel buckling tests, made available by Boeing Airplane Company, shows fair agreement with the theory used here. The test panels as constructed each had a different combination of values of k_t and core density. The test results, the face stress and the magnitude of q/b at which buckling occurred, are shown for each of the panels by the circled numbered points in Fig. 8. Each numbered curve in the same figure

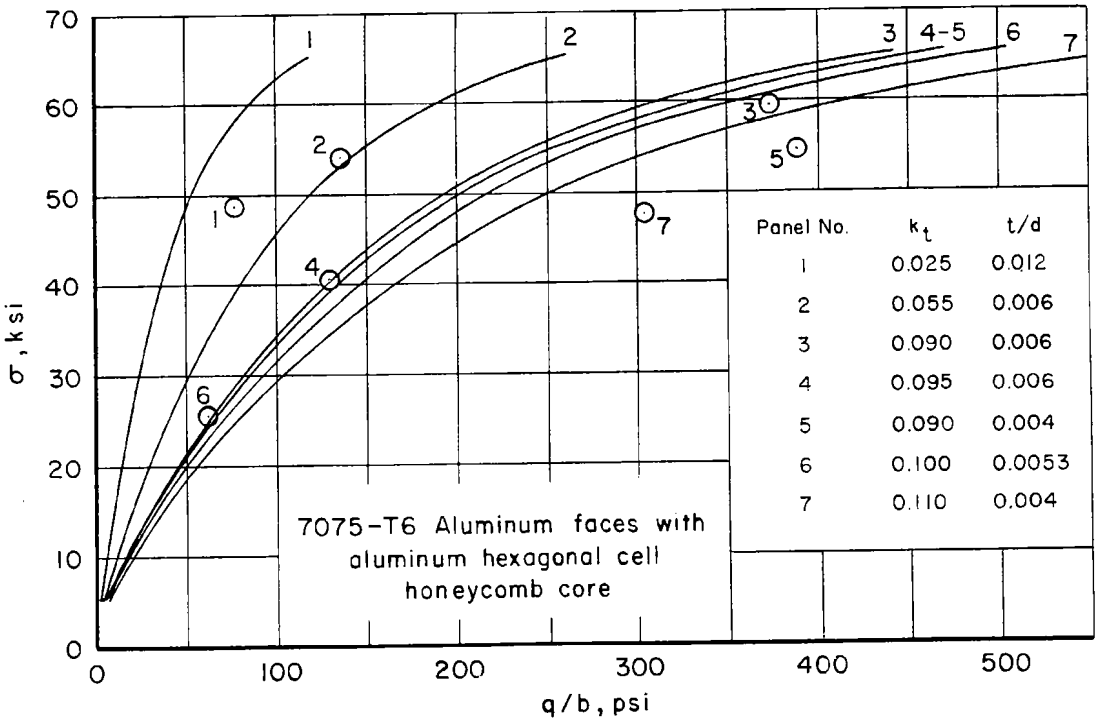

Fig. 8—Comparison of theoretical curves and results of Boeing tests

is a theoretical buckling curve, computed by using the value of k_t and core density corresponding to the panel whose test point is shown with the same number. The combinations of k_t and t/d were such that the approximation discussed in Appendix C was valid for all panels. Some of the disparity present may be due to material variations, since all curves were computed using a single stress-strain curve which was roughly representative of the several stress-strain curves obtained from test coupons of the face material in the test panels.

Suggestions For Further Experiments

The design method as presented here provides a rational basis for a more extensive, efficiently designed test program. Tests on panels of any configuration are useful in comparing theory with experiment, but it is particularly important to determine how closely theoretical envelope curves such as shown in Fig. 4 can be approached in practice. Consequently, it would be desirable to design test panels so that failure would be expected at points along the envelope curve, and this can be accomplished by choosing a value of b consistent with test facilities, selecting values of q to cover the desired range of q/b, and determining the proper values of face and core thickness for each value of q/b. This procedure could be repeated for each value of t/d desired. Tests of these panels would then show how well the envelope curves represent reality.

Investigation of some of the factors which may affect the level of the envelope curves can also be carried out. For example, an investigation of the effect of inelastic behavior might be conducted as follows. In Fig. 9 a buckling curve for a given face material, core material and configuration, and value of k_t is shown. The dashed curve is the buckling curve that would

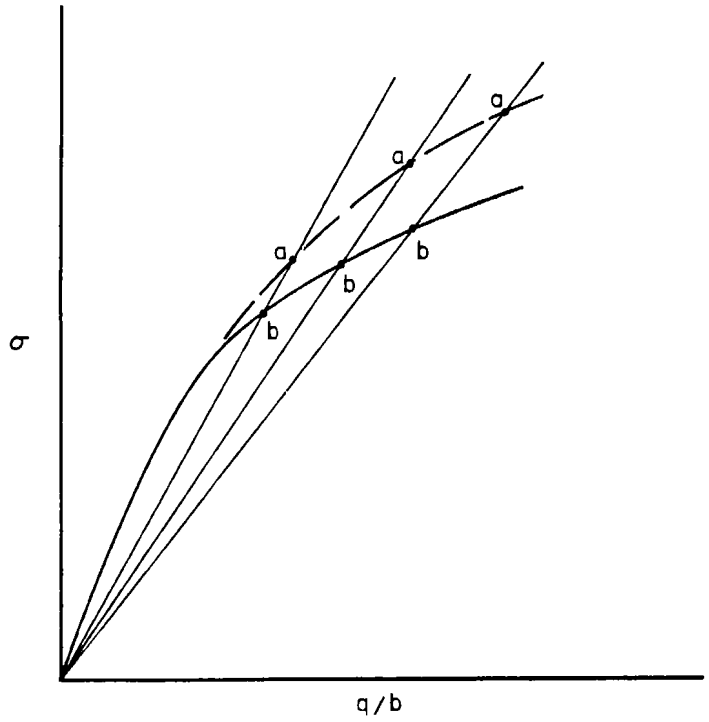

Fig. 9—Method of investigating effects of plasticity

obtain if the material were elastic over the full range of stress shown, while the solid curve results from an assumed form of the plastic reduction factor, η, e.g., $\sqrt{E_t/E}$. When a value of b is chosen, panels can be designed which would buckle at the points a on the elastic curve, if the material were to behave elastically. Then, as a panel is loaded, σ and q/b increase proportionally as indicated by the straight lines in the figure. If the panels actually buckle near the points b, the validity of the plastic reduction factor used is confirmed. If not, other forms of η should be investigated to find one that gives adequate agreement.

Similarly, to study wrinkling failure, a panel could be designed to fail at point a on the buckling curve shown in Fig. 10. The theoretical wrinkling stress for the material and value of t/d being considered is represented by the horizontal dashed line. Again, a test of the panel will demonstrate the accuracy of the wrinkling stress criterion used, although this information might be obtained more easily from short column tests.

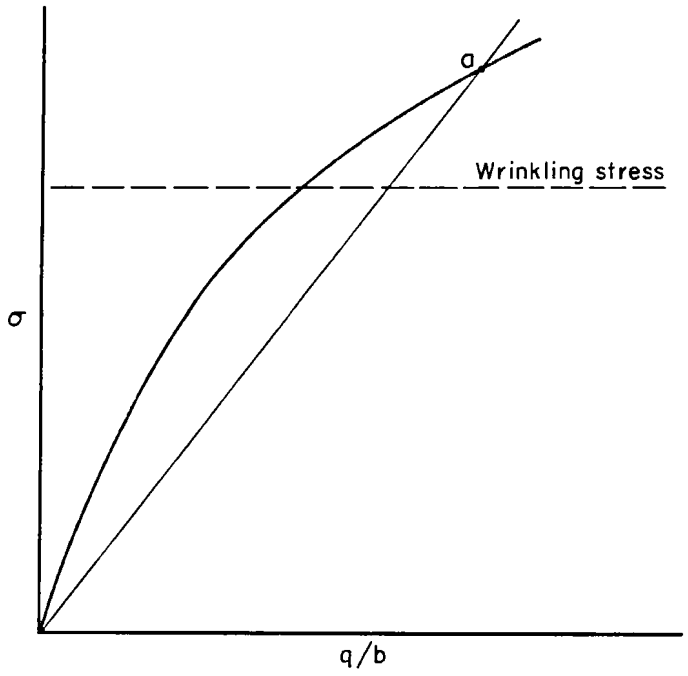

Fig. 10—Method for checking wrinkling stress

Extension of Method

Since the form of the buckling curves is a function of material properties, design curves for elevated temperature application can easily be obtained, at least for temperature ranges in which time effects are unimportant, merely by using the compressive stress-strain curve for the face material and the values of core shear moduli which apply at the desired temperature.

Investigation of sandwich panels with dissimilar core and face materials and with cores other than metallic honeycomb (e.g., foamed metal or plastic, or plastic impregnated fiberglass or asbestos honeycomb) can be easily accomplished by using the appropriate properties in the stress-structural index equation (Eq. 24) and in the equivalent stress equation (Eq. 21).

Extension to other loading and boundary conditions and other configurations, such as curved panels, can also be made for those cases for which satisfactory analysis equations are available.

If and when a design method, such as presented here, is shown to be reliable, the designer will be able to compare honeycomb panels with other

types of construction, considering weight, producibility, cost, etc., and make an informed choice.

Appendix A

CORE PROPERTIES

The mechanical properties (elastic moduli, density, crushing strength, etc.) of a honeycomb core may be expressed in terms of a dimensionless cell geometry parameter, t/d, where t is the thickness of the cell wall and d is related to cell size. Here, d is the diameter of an inscribed circle in the hexagonal or square cell. The properties referred to are "apparent" properties and describe behavior when core dimensions are much larger than cell dimensions so that inhomogeneity can be ignored.

Density

For honeycomb cores, the apparent density is the weight per unit volume, or $A_m \gamma_c / A_c$, where A_m is the area of metal associated with one cell, γ_c is the density of the cell wall material, and A_c is the area of a cell. Hexagonal cell honeycomb is manufactured with some double walls, and A_m in this case is $\frac{4dt}{\sqrt{3}}$. A_c is $\frac{\sqrt{3}\, d^2}{2}$, making the density $(8/3)(t/d)\gamma_c$. The density of aluminum cores is then $.26(t/d)\,lb/in^3$ or $450(t/d)\,lb/ft^3$. (Since the weight of adhesive used in making the core has been neglected, actual densities tend to be greater than predicted, particularly for cores made by pre-corrugating the foil. The densities of expanded cores, containing much less adhesive, agree quite well with predicted values.) A similar computation for square cell honeycomb leads to $2(t/d)\gamma_c$ for the density. Figure 11 shows a comparison of some measured values of density with the above relationships.*

*Experimental values of mechanical properties referred to in this appendix were obtained from Ref. 13 and from manufacturers' literature.

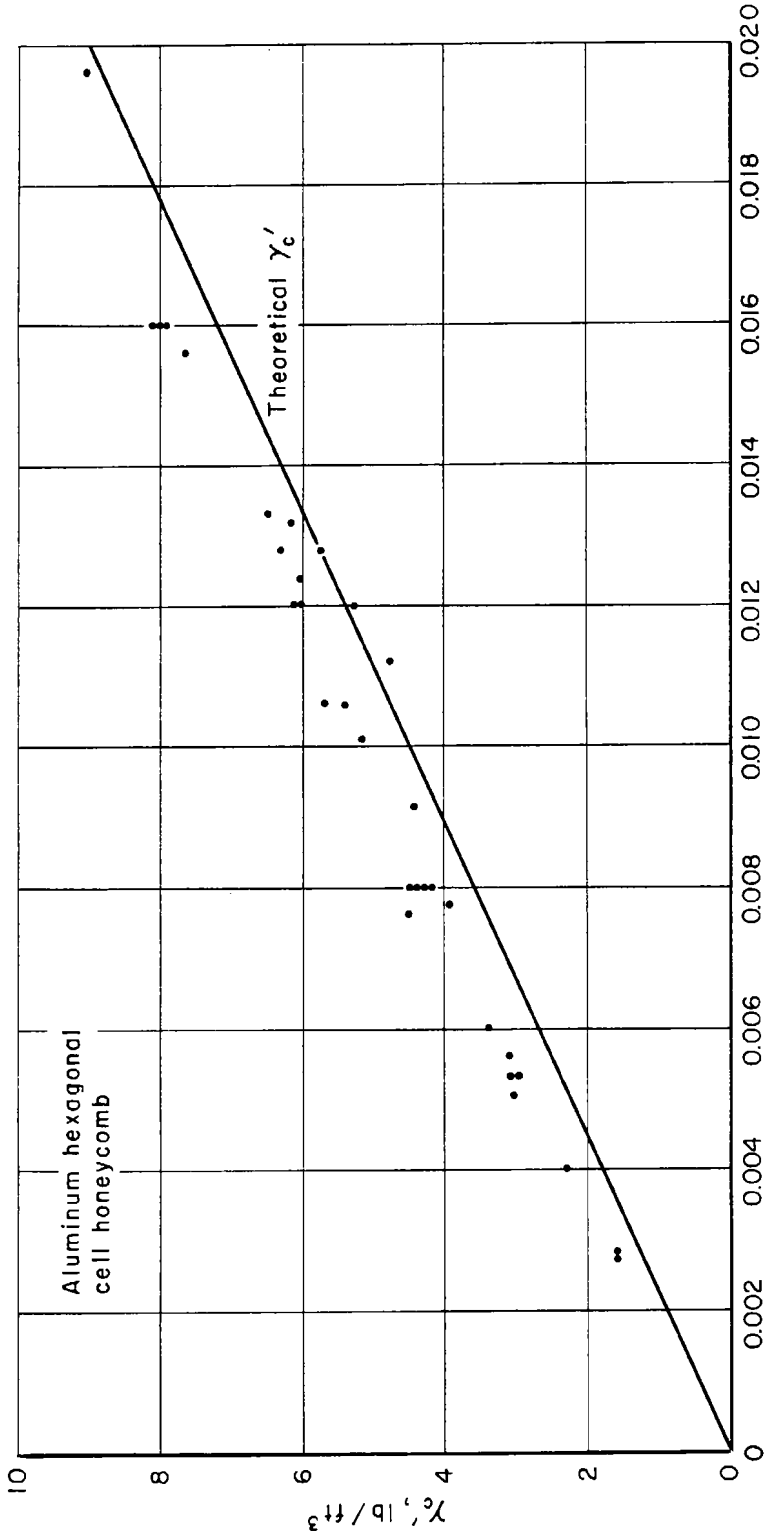

Fig. 11 — Comparison of theoretical and experimental values of apparent core density

Elastic Moduli

The apparent elastic modulus, E_c', in the direction of cell axes is simply the modulus of the core material, E_c, multiplied by A_m/A_c, or $(8/3)(t/d)E_c$ for hexagonal cells and $2(t/d)E_c$ for square cells.

The shear modulus varies with direction in an orthotropic material. The moduli of interest are those for the xz and yz planes, with axes as shown in Fig. 12. An approximate theoretical value for these moduli may be determined by considering shear only in the plane of the cell walls. If all points in the cell are given a displacement u in the x direction, $u = ay$, where a is a constant, the shear strain, γ, in the wall in the yz plane is a, and the shear stress, τ, in this wall is aG_c. In the angle walls, the shear strain is $a \cos 60^\circ = a/2$, and the shear stress is $aG_c/2$. Defining the apparent shear modulus in the yz plane as $G_{cx}' = \frac{\tau'}{\gamma}$ where τ' is the shear force per unit area of the core, we can determine G_{cx}'. The total shear force per cell in the x direction is

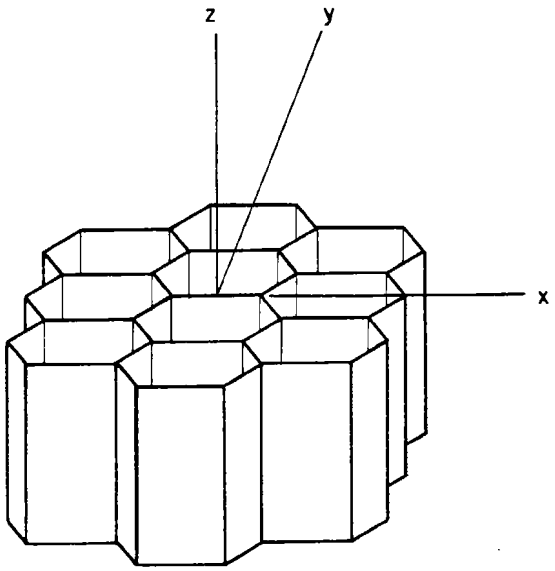

Fig. 12—Reference axes for hexagonal cells

$$2\tau t \frac{d}{\sqrt{3}} + 4 \frac{\tau}{2} \frac{t}{2} \frac{d}{\sqrt{3}} \cos 60^\circ = \frac{5}{2} \tau t \frac{d}{\sqrt{3}} = \frac{5}{8} \tau A_m = \frac{5}{8} A_m a G_c$$

Then

$$\tau' = \frac{5}{8} \frac{A_m}{A_c} aG_c$$

and

$$G'_{cx} = \frac{5}{8} \frac{A_m}{A_c} G_c = \frac{5}{3} \frac{t}{d} G_c$$

Repeating this procedure for the shear modulus in the yz plane gives

$$G'_{cy} = \frac{3}{8} \frac{A_m}{A_c} G_c = \frac{t}{d} G_c$$

As indicated in Fig. 13 experimental values of G'_{cx} agree fairly well with the above relationships, while experimental values of G'_{cy} are generally lower, and appear to be in the range of 0.4 G'_{cx} to 0.5 G'_{cx} instead of 0.6 G'_{cx} as predicted. The theoretical value has been used in this study, but in practice experimental values should be used.

The ideal square cell core is cylindrically aeolotropic with respect to the cell axes for shear moduli, and G'_{cx} and G'_{cy} should be the same. Again considering shear only in the plane of the cell walls, the apparent shear moduli are found to be $G'_{cx} = G'_{cy} = (t/d)G_c$. Little experimental data exists for checking these values. It appears that fabrication techniques may produce a difference in shear moduli in the x and y directions.

It is interesting to compare the properties of hexagonal and square honeycombs of equal density. In the region where the isotropic approximation may be used for hexagonal core, the effective shear modulus is $G'_{c\ eff} = \frac{2\ G'_{cx}\ G'_{cy}}{G'_{cx} + G'_{cy}}$. With the expressions for shear moduli developed previously, this becomes $\frac{2(5/3)(t/d)G_c(t/d)G_c}{(5/3)(t/d)G_c + (t/d)G_c} = (5/4)(t/d)G_c$. The effective shear

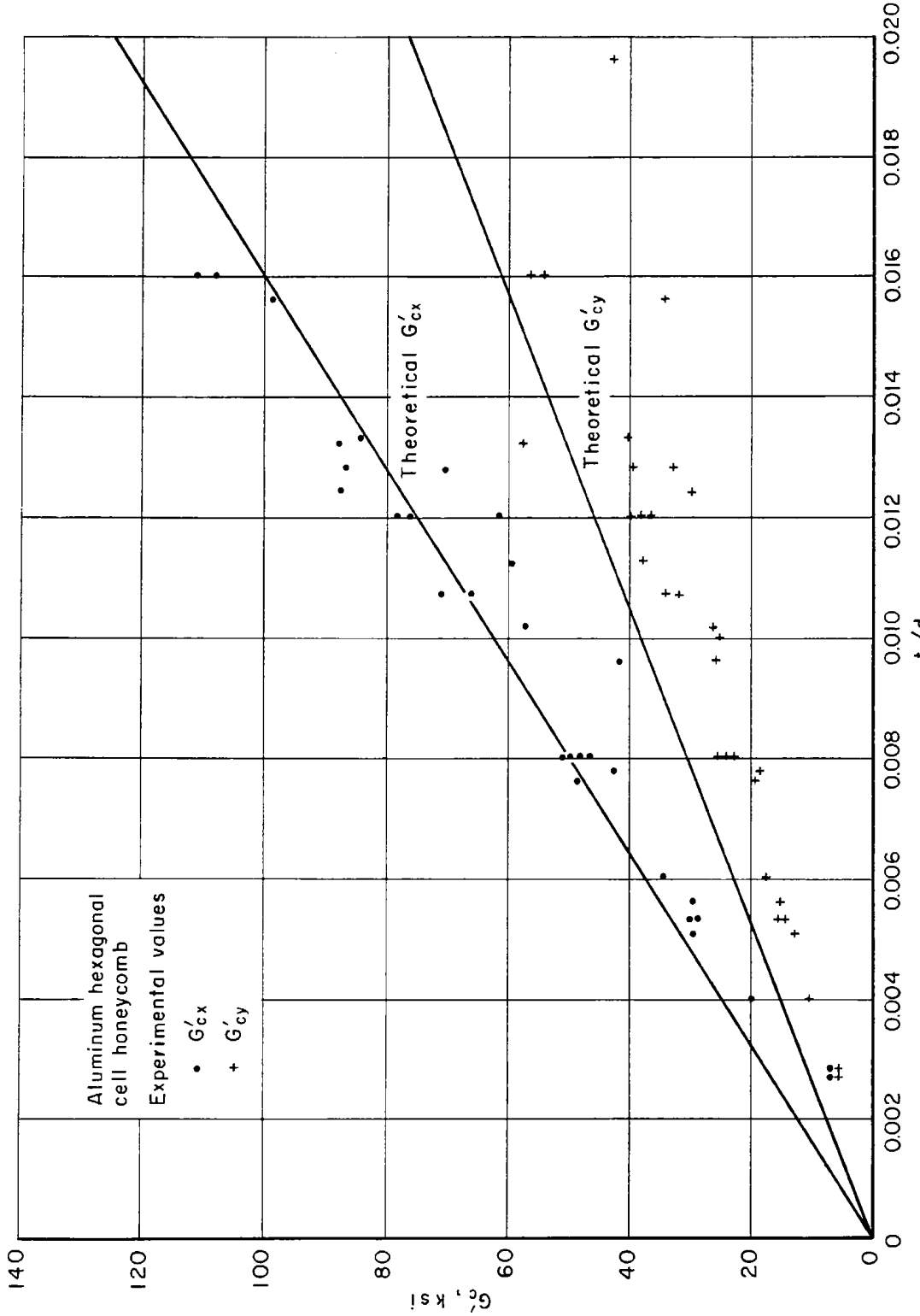

Fig. 13—Comparison of theoretical and experimental values of core shear moduli

modulus for the square cell is $(t/d)G_c$. For equal densities, $(8/3)(t/d)_{hex}\,\gamma_c = 2(t/d)_{sq}\,\gamma_c$, or $(t/d)_{hex} = (3/4)(t/d)_{sq}$. Then

$$G'_{c\ eff}(hex) = \frac{5}{4}\left(\frac{t}{d}\right)_{hex} G_c = \frac{15}{16}\left(\frac{t}{d}\right)_{sq} G_c, \text{ or } G'_{c\ eff}(hex) = .94\ G'_c\ (sq).$$

The shear modulus has a minor effect on buckling load in the region where this comparison is valid, hence the two types of core are very nearly equivalent. However, wrinkling stress and shear buckling stress, which depend on G'_{cx}, would be higher for the hexagonal cell core.

Appendix B

ADHESIVE WEIGHT

As mentioned previously, the effect of face-to-core adhesive weight on equivalent stress depends on the actual dimensions of the sandwich panel, and thus cannot be included on the proportion level. It will be shown here that the choice of optimum configuration is not affected by omission of this adhesive weight under certain conditions.

Denoting by σ^*_{eq} the equivalent stress when adhesive weight is considered

$$\sigma^*_{eq} = \frac{2f\sigma}{2f\frac{\gamma_f}{\gamma_r} + c\frac{\gamma'_c}{\gamma_r} + \frac{w_b}{\gamma_r}} = \frac{q}{2f\frac{\gamma_f}{\gamma_r} + c\frac{\gamma'_c}{\gamma_r} + \frac{w_b}{\gamma_r}}$$

With adhesive weight neglected

$$\sigma_{eq} = \frac{2f\sigma}{2f\frac{\gamma_f}{\gamma_r} + c\frac{\gamma_c}{\gamma_r}} = \frac{q}{2f\frac{\gamma_f}{\gamma_r} + c\frac{\gamma_c}{\gamma_r}}$$

or

$$2f\,\gamma_f/\gamma_r + c\,\gamma_c/\gamma_r = q/\sigma_{eq}$$

Thus

$$\sigma^*_{eq} = \frac{q}{q/\sigma_{eq} + w_b/\gamma_r}$$

At a given q and b, we wish to evaluate the effect of adhesive weight on the choice of optimum configuration. In Fig. 14, curves 1 and 2 are buckling curves which may be for different materials, different values of

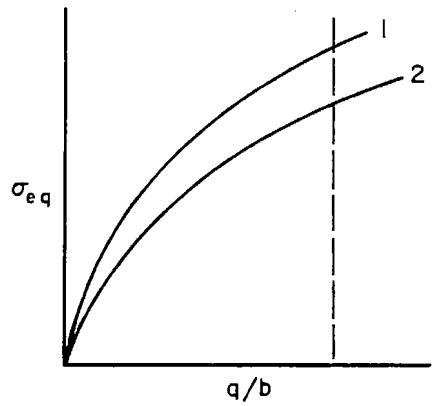

Fig. 14 — σ_{eq}-q/b curves for bonding weight discussion

k_t, and different types of core. At the given q/b, curve 1 appears to result in lighter construction, since $\sigma_{eq\ 1} > \sigma_{eq\ 2}$. With adhesive weight included

$$\frac{\sigma^*_{eq\ 1}}{\sigma^*_{eq\ 2}} = \frac{q/\sigma_{eq\ 2} + w_{b2}/\gamma_r}{q/\sigma_{eq\ 1} + w_{b1}/\gamma_r}$$

Here q/σ_{eq} is the equivalent thickness of the reference material with bonding weight neglected, and w_b/γ_r is the equivalent thickness of bonding material. Therefore

$$\frac{\sigma^*_{eq\ 1}}{\sigma^*_{eq\ 2}} = \frac{t_{r2} + t_{b\ eq\ 2}}{t_{r1} + t_{b\ eq\ 1}}$$

Hence, if the adhesive weight is the same in each case, (or if $w_{b2} > w_{b1}$), the σ_{eq} versus q/b curves give a true indication of which type of panel would be lighter for any value of q/b. If $w_{b1} > w_{b2}$, as might be the case if a brazed steel sandwich is to be compared with an adhesive bonded aluminum sandwich, the σ_{eq} versus q/b curves may not give an accurate picture of relative weights, particularly for low values of q, for which the weight of bond material may become an appreciable part of the total weight of the panel. However, for given values of q, σ_{eq}, and w_b, the effect of adhesive weight can be easily determined. In cases where comparison of sandwich with other types of construction is desired, σ_{eq} is in general a valid basis of comparison, as long as adhesive weight is small compared with skin and core weight, but the possible effect of adhesive weight should be kept in mind.

Appendix C

APPROXIMATION FOR ORTHOTROPIC CORES

An approximation has been made which allows computation of buckling curves for sandwich panels with orthotropic cores by means of equations developed for isotropic cores. The conditions under which this approximation is acceptable will be discussed here.

As noted previously, the equation for buckling load for the orthotropic core sandwich panel is

$$\frac{qb^2}{\pi^2 B} = \frac{\left[\lambda s_x s_y + a\,(s_x + \lambda s_y)\right]\quad (1+\lambda)^2}{\lambda s_y + \lambda^2 s_x + \lambda^2 s_x s_y + a\lambda\,(s_x + \lambda s_y) + a\,(1+\lambda)^2}$$

or denoting the right hand side of the equation by K_o, $\frac{qb^2}{\pi^2 B} = K_o$. For an isotropic core, $s_x = s_y = s$, and the right hand side will be denoted by K_i. With the value of λ which minimizes it, $K_i = \frac{4s^2}{(1+s)^2}$. Now $\frac{qb^2}{\pi^2 B} = \frac{qs_x}{S_x} = \frac{2s_x k_t \sigma}{(1+k_t)^2 G'_{cx}}$. Letting

$$\bar{\sigma} = \frac{2k_t \sigma}{(1+k_t)^2 G'_{cx}} \tag{25}$$

we have $\bar{\sigma} = K_o/s_x$ for the orthotropic core and $\bar{\sigma} = \frac{4s}{(1+s)^2}$ for the isotropic core. Further, $s_x = \frac{8 G'_{cx} (1-\nu^2) k_t \sigma^2}{\pi^2 E\eta (q/b)^2}$. Letting $\overline{q/b} = \frac{2k_t}{(1+k_t)^2 G'_{cx}} \sqrt{\frac{\pi^2 E\eta}{8 G'_{cx} (1-\nu^2) k_t}}$, $s_x = \frac{\bar{\sigma}^2}{(\overline{q/b})^2}$, or $\overline{q/b} = \frac{\bar{\sigma}}{\sqrt{s_x}}$. We can now plot curves of $\bar{\sigma}$ versus $\overline{q/b}$ for the isotropic core as shown in Fig. 15 by using the parametic equations in s (or the buckling equation, Eq. (24) can be written $\overline{q/b} = \sqrt{\bar{\sigma}}\left(1 - \sqrt{1-\bar{\sigma}}\right)$.)

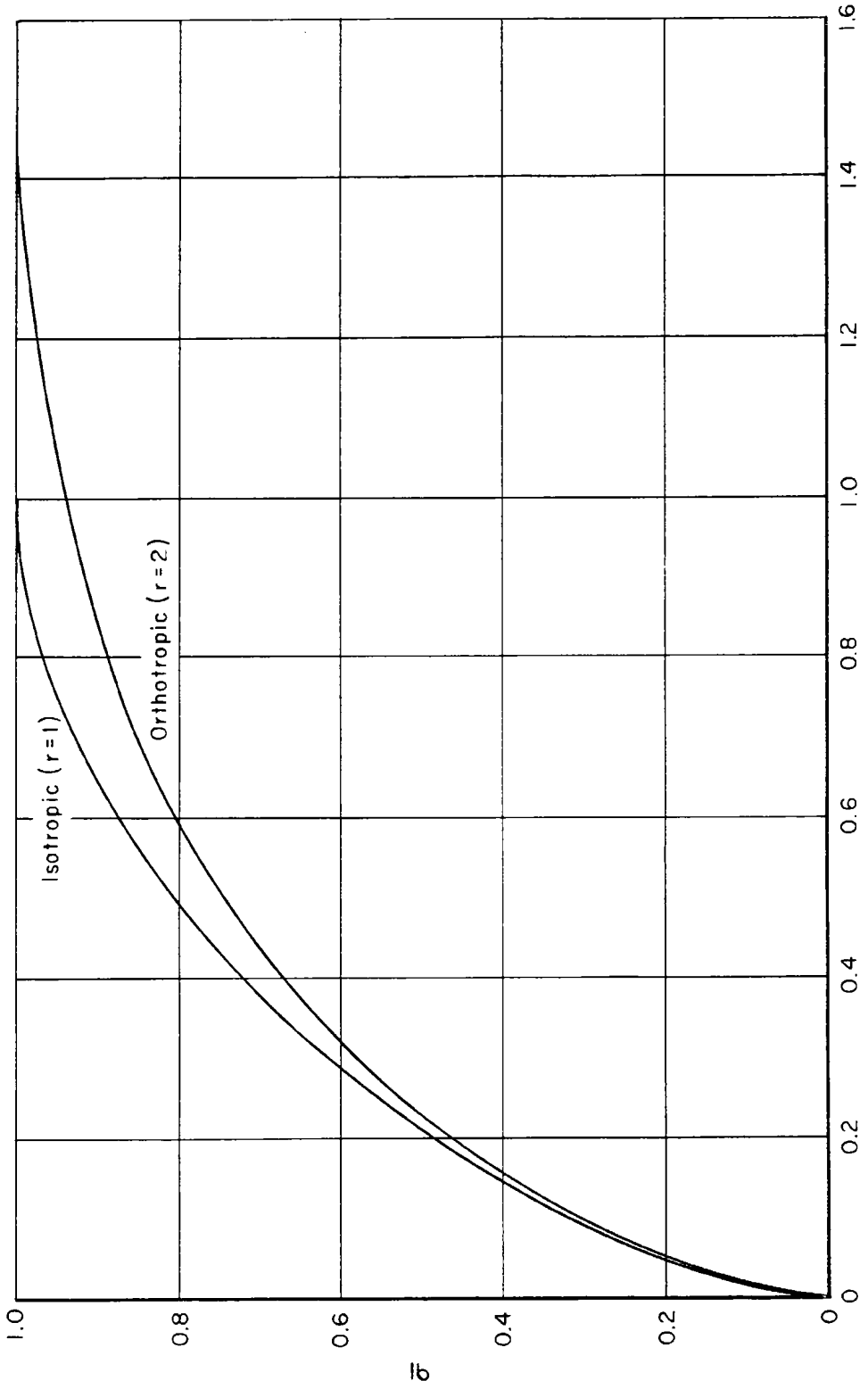

Fig. 15 — Non-dimensional buckling curves

For the orthotropic core, the λ which minimizes K_o for a given s_x and s_y must be determined. The $\bar{\sigma} - \overline{q/b}$ curves in Fig. 15 for $r = 2$ ($s_x = 2s_y$) were obtained from values of K_o which were computed using values of λ given by Plantema.

It has been assumed that the orthotropic case can be treated by considering it isotropic, with an effective shear modulus $G'_{c\ eff} = \frac{2\ G'_{cx}}{1 + r}$, or with $r = 2$, $G'_{c\ eff} = \frac{2}{3} G'_{cx}$. The effect of this approximation can be shown with the aid of the $\bar{\sigma} - \overline{q/b}$ relationship. Since the actual face stress is given by $\sigma = \frac{(1 + k_t)^2\ G'_{cx}\ \bar{\sigma}}{2k_t}$, making a comparison at the same face stress means that $\frac{(1 + k_t)^2\ G'_{cx}\ \bar{\sigma}_o}{2k_t} = \frac{(1 + k_t)^2\ G'_{c\ eff}\ \bar{\sigma}_i}{2k_t}$, or for a given k_t, $\bar{\sigma}_o$ corresponds to $\bar{\sigma}_i \frac{G'_{c\ eff}}{G'_{cx}} = \bar{\sigma}_i \frac{2}{1 + r}$. By the same token, using the relationship

$$\overline{q/b} = \frac{\bar{\sigma}}{\sqrt{s_x}} = \frac{2\pi k_t}{(1 + k_t)^2} \sqrt{\frac{E\eta}{8\ (1 - \nu^2)\ k_t}}\ \frac{q/b}{(G'_{cx})^{3/2}} \qquad (26)$$

it is apparent that for the same value of q/b, $(\overline{q/b})_o$ corresponds to $\left(\frac{G'_{c\ eff}}{G'_{cx}}\right)^{3/2} (\overline{q/b})_i = \left(\frac{2}{1 + r}\right)^{3/2} (\overline{q/b})_i$. Thus, for $r = 2$, a plot of $(2/3)\ \bar{\sigma}_i$ versus $.544\ (\overline{q/b})_i$ superposed on the $\bar{\sigma}_o - (\overline{q/b})_o$ plot for $r = 2$ permits a comparison referred to the actual σ and q/b. This is shown in Fig. 16, from which it is apparent that the approximation is conservative and that it may be used for values of $\bar{\sigma}_o$ up to about .63 with less than 5% error, i.e., for values of σ, G'_{cx} and k_t such that $\frac{2\sigma k_t}{(1 + k_t)^2\ G'_{cx}} \leq .63$.

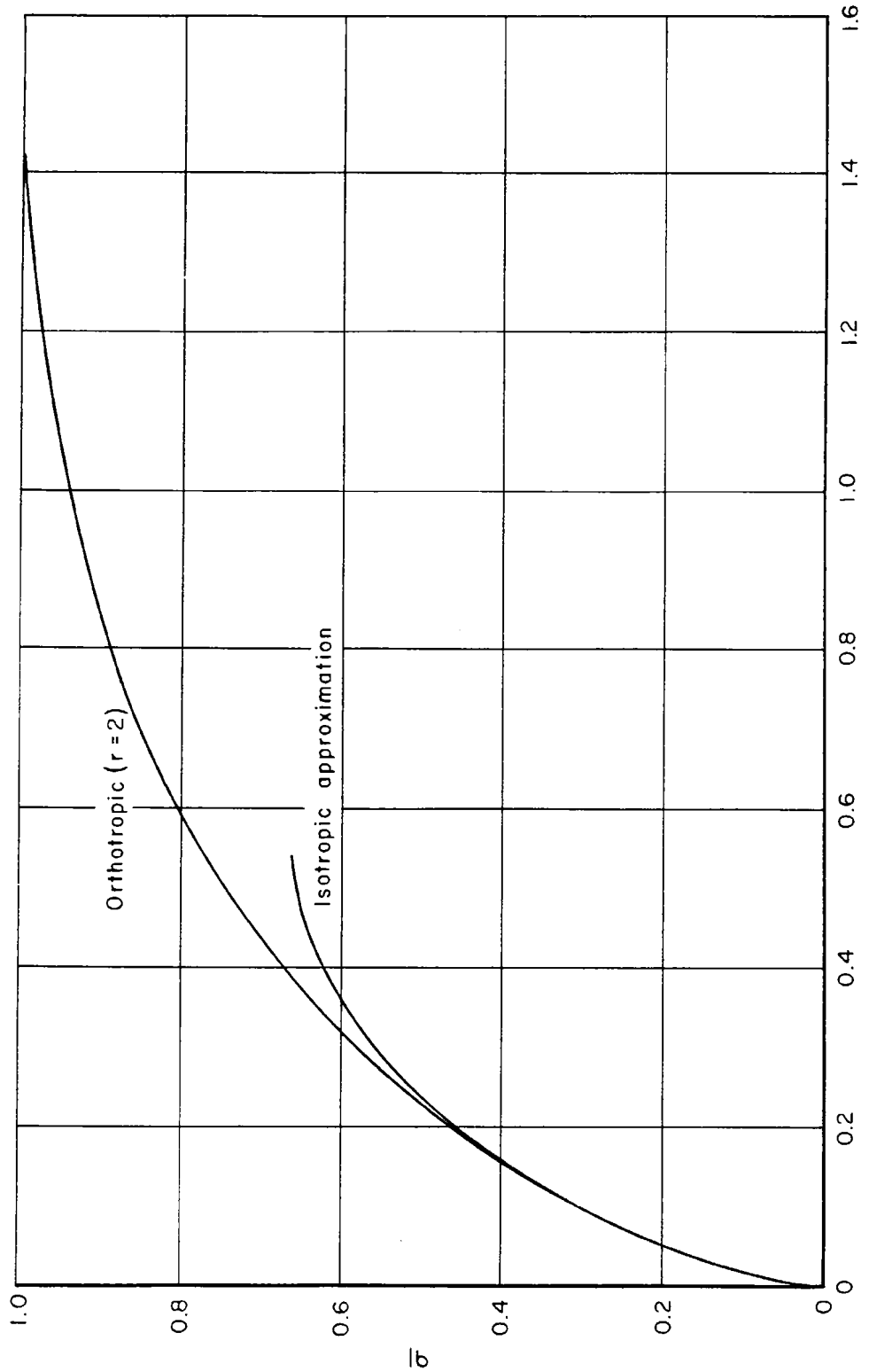

Fig. 16 — Non-dimensional buckling curves for evaluation of approximation discussed in appendix C

The approximation is better, of course, for values of r closer to one. Buckling curves for values of $\bar{\sigma}_o$ above the range of validity of the approximation discussed here may be obtained (for r = 2) as follows: choose a value of σ, for given values of G'_{cx} and k_t, find $\bar{\sigma}$ from Eq. 25, get $\overline{q/b}$ from the curve for r = 2 in Fig. 15, and with the value of η determined by the chosen value of σ compute q/b from Eq. 26. This procedure might be adapted to machine computation by approximating the curve in Fig. 15 with a polynomial.

Appendix D

WRINKLING

In the foregoing work, failure modes other than quasi-Euler buckling were mentioned only in passing, primarily because of the present state of knowledge concerning these modes. A considerable amount of theoretical work has been done on wrinkling failure, particularly for faces supported by continuous cores, but there exists some question whether this work is applicable to honeycomb core panels.

For continuous cores, the simplest expressions for wrinkling stress result from energy derivations in which it is assumed that only part of the core is involved when the face wrinkles. The wrinkling stress in this case as given by different investigators is $\sigma_{wr} = K \sqrt[3]{E_f E'_c G'_c}$, where K is a constant, E_f is the elastic modulus of the face, E'_c is the apparent elastic modulus of the core in a direction normal to the faces, and G'_c is the apparent shear modulus of the core in a plane normal to the faces and parallel to the load. Hoff and Mautner[1] give K the value 0.91, but suggest the use of 0.5. Williams[14] finds a K of 0.85 (if the elastic modulus of the core in a direction parallel to the load is negligibly small). Yusuff[15] gives 0.961 and he shows that the work of Gough, Elam and De Bruyne[16] results in a K of 0.78, with certain assumptions for Poisson's ratio and the shear modulus.

For cases in which the entire core is affected by face wrinkling, Hoff and Mautner predict an increase in σ_{wr} as k_t increases, while Yusuff's results indicate first a decrease and then an increase as k_t increases. Goodier and Hsu[17] consider several possible modes of wrinkling, and find that k_t influences the wrinkling stress in all cases. Norris, Ericksen,

March, Smith, and Boller,[18] in a rather extensive investigation, discuss wrinkling of faces supported by a continuous core, and include such effects as the magnitude of k_t, initial irregularities in the faces, and shear and tensile strength of the core or face-to-core bond. Norris, Boller and Voss[19] extend this work to honeycomb-core sandwich and conclude from experiments with resin-treated paper honeycomb core with steel faces that cell size may have an appreciable effect on the wave length of wrinkles and hence on wrinkling stress. By use of their expression for wrinkling stress which includes wave length and the tensile strength of the face-to-core bond (or of the core) divided by the ratio of the amplitude to half wavelength of the initial deformation of the face as parameters, fair agreement with experiment was obtained when these parameters were determined empirically from the experiments. The possibility is mentioned that this procedure may give fictitious values of the parameters mentioned which merely produce a smooth curve through experimental points. It appears that more experimental work on wrinkling needs to be done and compared with various theories before wrinkling stress can be successfully predicted.

The proper method of including the effect of inelastic behavior of the faces is not well-defined, although a reduced modulus is suggested in Ref. (18). Further complication arises in assessing possible changes in the core moduli when face stresses exceed the elastic limit.

A rough indication of the magnitude of wrinkling stress for honeycomb core sandwich is given in Fig. 17, in which wrinkling stress is plotted against t/d for aluminum, titanium, and steel square- and hexagonal-cell honeycomb sandwich. The wrinkling stress was computed from the expression suggested by Hoff and Mautner, $\sigma_{wr} = .5 \sqrt[3]{E_f E_c' G_{cx}'}$, modified for the

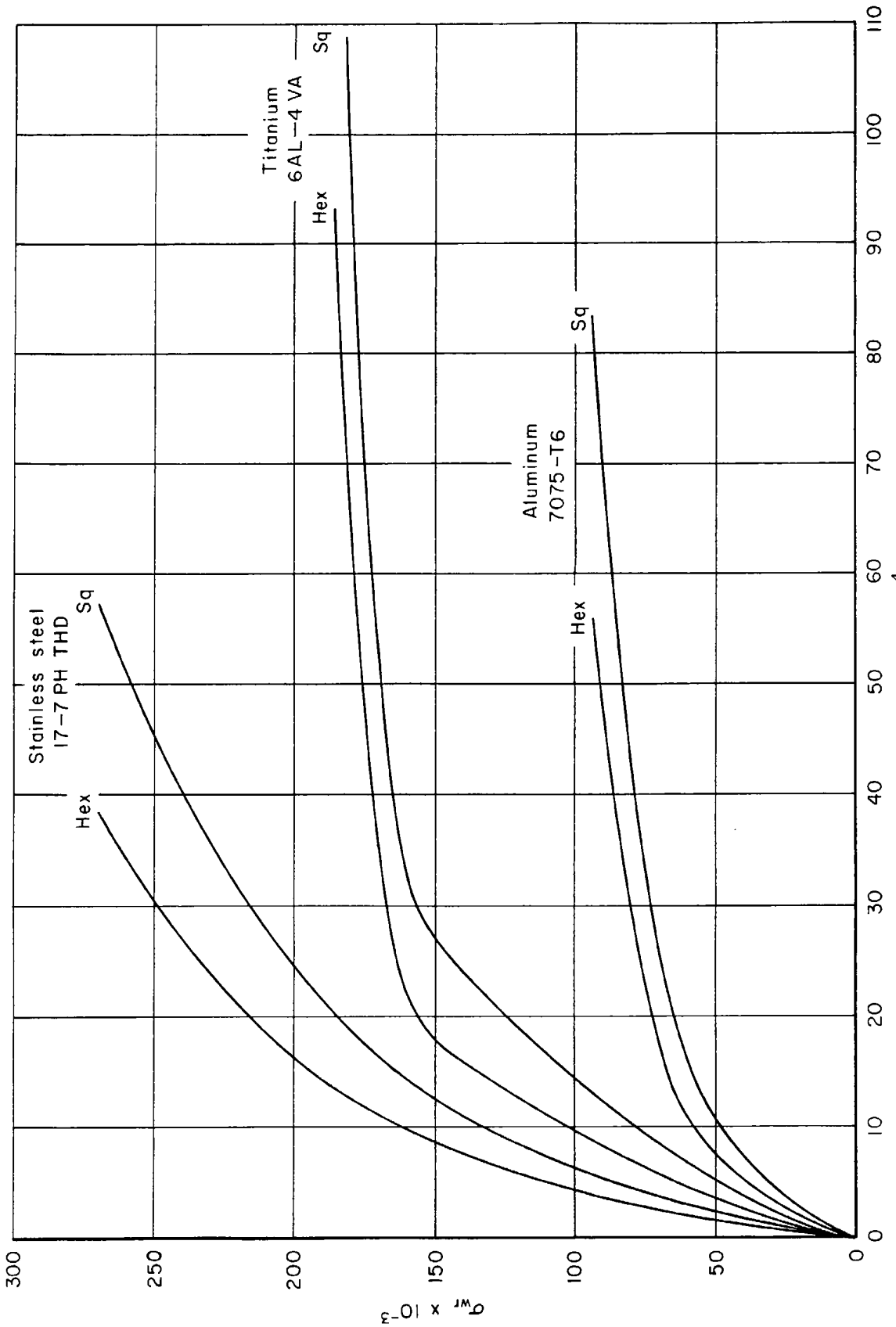

Fig. 17—Wrinkling stress vs t/d for faces supported by honeycomb cores

inelastic region by replacing E_f with $E_f\eta$, where $\eta = \sqrt{E_t/E_f}$. Values of apparent core moduli were obtained from the expressions developed previously.

Commercially available honeycomb core ranges from t/d = .001 to t/d = .016 for stainless steel square cell, from t/d = .0027 to t/d = .016 for aluminum hexagonal cell, and from t/d = .004 to t/d = .016 (predicted) for titanium square cell. Thus it is apparent that in most cases the face stress will probably be limited by considerations other than wrinkling stress.

Appendix E

MONOCELL BUCKLING

Norris and Kommers[20] investigated monocell buckling (or dimpling) and found experimental evidence indicating that the critical stress for this type of instability is given approximately by $\sigma_{mc} = .9\ E_r\ (f/d)^{3/2}$, where E_r is a reduced modulus, $E_r = \frac{4\ E_f\ E_t}{\left(\sqrt{E_f} + \sqrt{E_t}\right)^2}$, f is the face thickness, and d is the diameter of a circle inscribed in the cell. (Use of the tangent modulus E_t, in place of E_r results in a more conservative value of σ_{mc}.) The tests were made with solid cores with a hole drilled through them to simulate a cell, and with one type of impregnated-paper hexagonal-cell honeycomb, both with aluminum faces. Application of this equation to metallic hexagonal- and square-cell honeycomb with various cell sizes and foil thicknesses should probably be verified by further tests.

Assuming that σ_{mc} may be predicted with sufficient accuracy by the above expression, with $f = q/2\ \sigma_{mc}$ and using the tangent modulus, it may be rewritten as $\sigma_{mc} = .9\ E_t \left[q/(2\ \sigma_{mc}\ d)\right]^{3/2}$, or $q/d = \frac{2.15\ \sigma_{mc}^{5/3}}{E_t^{2/3}}$. Then curves of σ_{mc} versus q/d can be plotted, as in Fig. 18, and for a given q the value of d necessary to prevent monocell buckling at a given stress may be determined; or, alternatively, if available values of cell size are limited, the monocell buckling stress for the smallest available cell size can be determined. This stress would then be used as a cut-off stress analogous to the stress limitation resulting from minimum gage considerations.

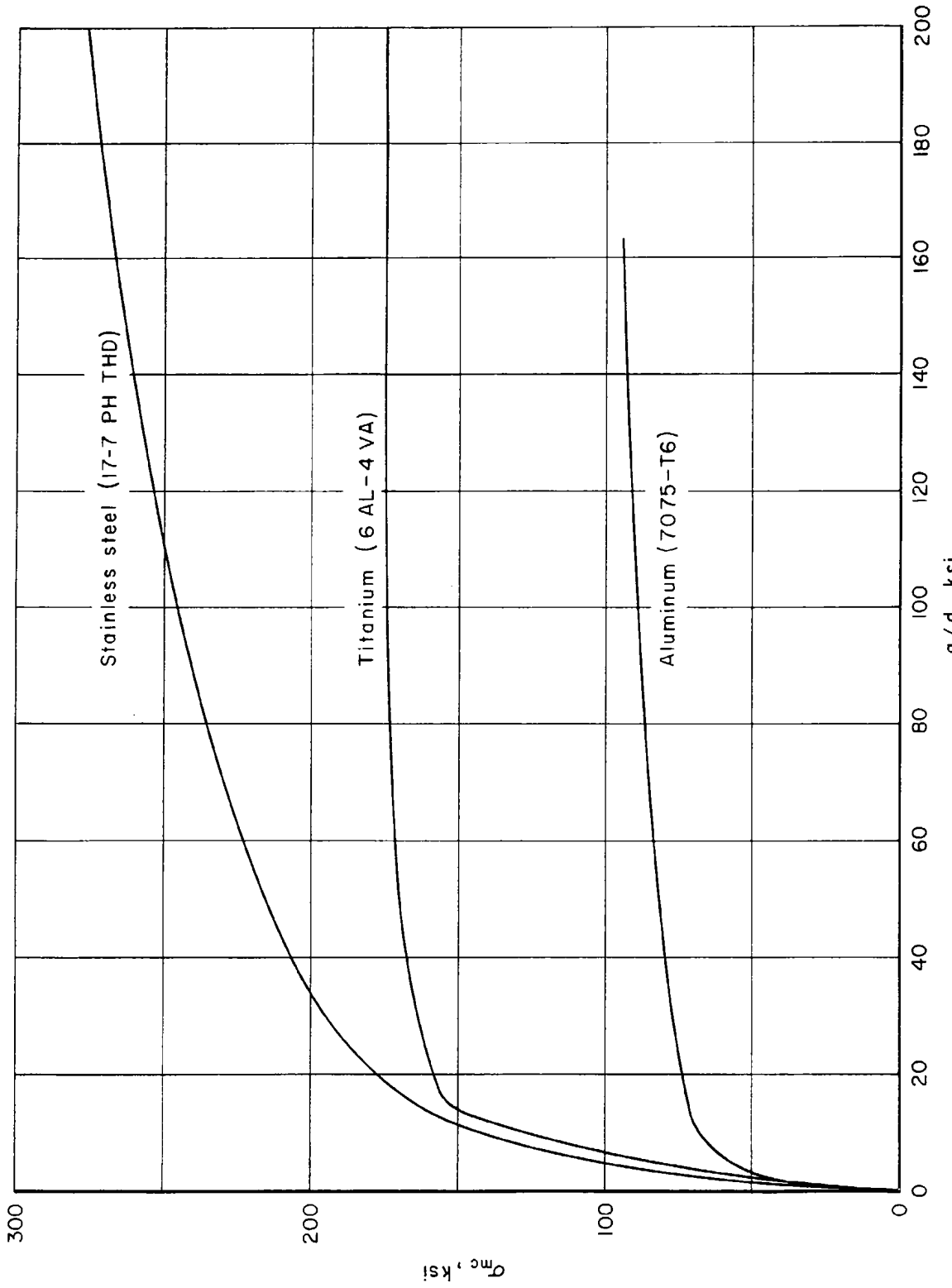

Fig. 18 — Monocell buckling stress vs q/d

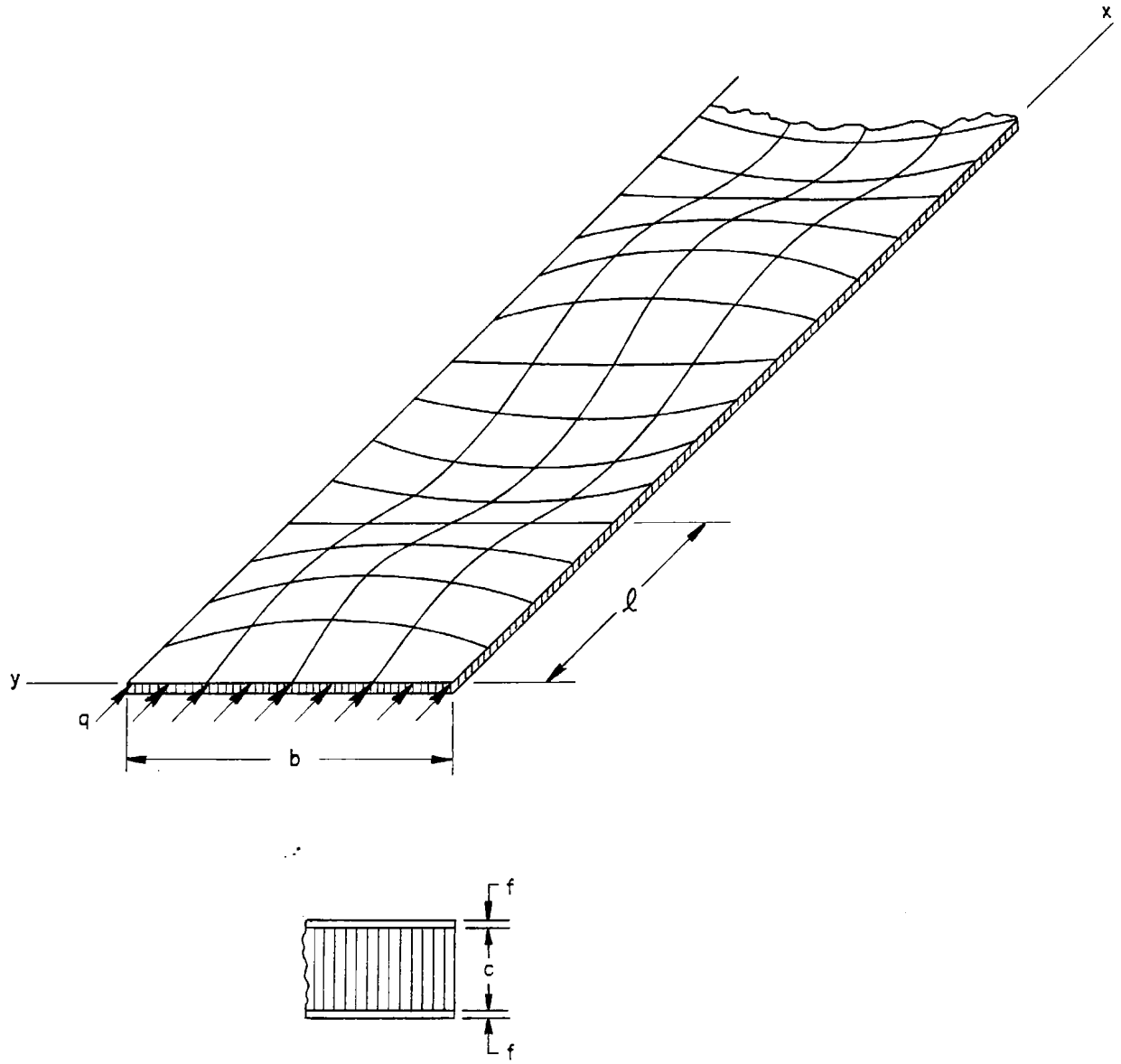

Fig. 19 — Panel geometry

LIST OF SYMBOLS

$a = \frac{1 - \nu}{2}$

B = bending stiffness, $\frac{E_f f (f + c)^2}{2 (1 - \nu^2)}$

b = width of panel (see Fig. 19)

c = core thickness

d = diameter of inscribed circle in honeycomb cell

E = Young's modulus

f = face thickness

G = shear modulus

k_t = face to core thickness ratio, f/c

ℓ = half wave length of buckles

q = axial load on panel per unit width

$r = S_x/S_y = s_x/s_y = G'_{cx}/G'_{cy}$

S = shear stiffness, $\frac{(c + f)^2 G'_c}{c}$

s = relative shear stiffness parameter, $\frac{b^2 S}{\pi^2 B}$

t = thickness of foil in honeycomb cell walls

η = plasticity reduction factor

$\lambda = \ell^2/b^2$

ν = Poisson's ratio of face material

σ = compressive stress in faces

SUBSCRIPTS:

c = core properties

f = face properties

i = isotropic core

o = orthotropic core

x, y = coordinate directions (see Fig. 19)

Primed quantities refer to apparent core properties.

REFERENCES

1. Hoff, N. J. and S. E. Mautner,"The Buckling of Sandwich-Type Panels," Journal Of The Aeronautical Sciences, Vol. 12, No. 3, p. 285, July 1945.

2. Libove, Charles and S. B. Batdorf, A General Small-Deflection Theory for Flat Sandwich Plates, NACA TN 1562, April 1948.

3. Ericksen, Wilhelm S. and H. W. March, Effects of Shear Deformation in the Core of a Flat Rectangular Sandwich Panel, Forest Products Laboratory Report No. 1583-B, November 1950.

4. Plantema, F. J., Theory and Experiments on the Elastic Overall Instability of Flat Sandwich Plates, Thesis, Technical Institute of Delft, May 1952.

5. Bijlaard, P. P.,"Analysis of the Elastic and Plastic Stability of Sandwich Plates by the Method of Split Rigidities - I," Journal of the Aeronautical Sciences, Vol. 18, No. 5, p. 339, May 1951.

6. Hoff, N. J., Bending and Buckling of Rectangular Sandwich Plates, NACA TN 2225, November 1950.

7. Seide, Paul and Elbridge Z. Stowell, Elastic and Plastic Buckling of Simply Supported Metalite Type Sandwich Plates in Compression, NACA TN 1822, February 1949.

8. Johnson, Aldie E., Jr. and Joseph W. Semonian, A Study of the Efficiency of High-Strength, Steel, Cellular-Core Sandwich Plates in Compression, NACA TN 3751, September 1956.

9. Stowell, Elbridge Z., A Unified Theory of Plastic Buckling of Columns and Plates, NACA Report 898, 1948.

10. Shanley, F. R., Weight-Strength Analysis of Aircraft Structures, The RAND Corporation, Report R-222, July 1952.

11. Flugge, W., "The Optimum Problem of the Sandwich Plate," Journal of Applied Mechanics, Vol. 19, No. 1, p. 104, March 1952.

12. Micks, W. R., "A Method of Estimating the Compressive Strength of Optimum Sheet-Stiffener Panels for Arbitrary Material Properties, Skin Thickness, and Stiffener Shapes," Journal of the Aeronautical Sciences, Vol. 20, No. 10, p. 705, October 1953.

13. Kuenzi, Edward W., Mechanical Properties of Aluminum Honeycomb Cores, Forest Products Laboratory Report No. 1849, September 1955.

14. Williams, D., Sandwich Construction - A Practical Approach for the Use of Designers, Aeronautical Research Council, R and M No. 2466, April 1947.

REFERENCES (cont'd)

15. Yusuff, Syed, "Theory of Wrinkling in Sandwich Construction", Journal of the Royal Aeronautical Society, Vol. 59, No. 529, p. 30, January 1955.

16. Gough, C. S., C. F. Elam and N. A. De Bruyne, "The Stabilization of a Thin Sheet by a Continuous Supporting Medium," Journal of the Royal Aeronautical Society, Vol. 44, No. 349, p. 12, January 1940.

17. Goodier, J. N. and C. S. Hsu, "Nonsinusoidal Buckling Modes of Sandwich Plates," Journal of the Aeronautical Sciences, Vol. 21, No. 8, p. 525, August 1954.

18. Norris, Charles B., Wilhelm S. Ericksen, H. W. March, C. B. Smith and Kenneth H. Boller, Wrinkling of the Facings of Sandwich Construction Subjected to Edgewise Compression, Forest Products Laboratory, Report No. 1810, November 1949.

19. Norris, Charles B., Kenneth H. Boller, and Arnold W. Voss, Wrinkling of the Facings of Sandwich Construction Subjected to Edgewise Compression, Sandwich Constructions Having Honeycomb Cores, Forest Products Laboratory Report No. 1810-A, June 1953.

20. Norris, C. B. and W. J. Kommers, Short-Column Compressive Strength of Sandwich Constructions as Affected by the Size of the Cells of Honeycomb-Core Materials, Forest Products Laboratory Report No. 1817, August 1950.